A new averaging-extrapolation method for quasi-periodic frequency refinement*

Jordi Villanueva†

Departament de Matemàtiques,

Universitat Politècnica de Catalunya,

Diagonal 647, 08028 Barcelona (Spain).

March 23, 2022

Abstract

In a recent work, we presented an averaging-extrapolation approach for the numerical computation of frequencies and amplitudes of a discrete-time quasi-periodic signal. This approach assumes analyticity of the signal and a Diophantine frequency vector. Given an approximation to one of the frequencies and a sufficiently large number of iterates of the signal, the main outcome of the method is a refined approximation to the frequency. The crucial aspect of this method consists in building an appropriate complex signal which, by the geometrical implications of its construction, is referred to as an unfolded signal. The projection of the unfolded signal on the unit circle defines a quasi-periodic signal of the circle whose rotation frequency is the target frequency. This allows to refine the target frequency by adapting a previously developed method for computing, with great accuracy, Diophantine rotation numbers of analytic circle maps. Both the unfolding and refinement processes require computing appropriate weighted averages of the iterates and performing Richardson's extrapolation. In the present work, we reformulate this averaging-extrapolation approach to frequency refinement. This leads to a simpler method that completely avoids the unfolding process but that is capable of producing accurate values for frequencies and amplitudes at a reasonable computational cost, which is mostly independent of the number of basic frequencies of the signal.

PACS: 02.30.Mv; 02.60.-x; 02.70.-c.

MSC: 37C55; 37E45; 37J10; 37J40; 37M10; 65Txx; 70K43;

Keywords: Quasi-periodic signal; Quasi-periodic frequency analysis; Numerical approximation; Invariant tori.

*This work has been partially supported by the Catalan grant 2017SGR1049 and the Spanish MINECO-FEDER Grant PGC2018-098676-B-100 (AEI/FEDER/UE).

†E-mail: jordi.villanueva@upc.edu; web-page: https://www.mat.upc.edu/en/people/jordi.villanueva

1 Introduction

When modelling applied problems of science and technology through dynamical systems, several naturally arising questions are concerned with the long-time behaviour of the solutions of the system. In many contexts, quasi-periodic solutions are crucial when studying this long-time behaviour, both for continuous-time and discrete-time systems. This assertion is mainly relevant in Hamiltonian systems and in symplectic maps, although quasi-periodic solutions are also natural objects of interest in many other contexts (e.g., in dissipative ordinary differential equations). From the perspective of applications, quasi-periodic solutions play a central role, e.g., in celestial mechanics, astrodynamics, molecular dynamics, and plasma-beam physics. The interested reader is referred to [1, 2, 5] and references therein for a wider picture of quasi-periodicity in dynamical systems.

A quasi-periodic solution of a dynamical system densely fills a torus invariant by the motion. In this work, we are concerned with quasi-periodic invariant tori with normal stable behaviour or, at least, with a region of effective stability around them. By effective stability we mean stability from the practical viewpoint. E.g., it is known that maximal dimensional tori and normally elliptic lower-dimensional tori of Hamiltonian systems are very sticky, so that nearby solutions remain close to them for a very long time (see, e.g., [9]). Therefore, we will assume that the time evolution of the considered quasi-periodic motions can be numerically followed, with high accuracy, over very long time spans. This assumption is basic to justify the effectiveness of averaging-extrapolation methods for frequency analysis.

As a starting point, we assume that a finite sequence of iterates of a discrete-time quasi-periodic signal is known (see definition 2.1). This sample of the signal may come from the iteration of an appropriate initial condition by a discrete-time dynamical system or from a continuous-time quasi-periodic signal evaluated at equally spaced times. The introduction to [15] discusses various ways of generating quasi-periodic signals which meet the requirements of our approach. The process that numerically computes frequencies and amplitudes of a quasi-periodic signal from this finite sample is called quasi-periodic frequency analysis. Knowing the amplitudes provides a Fourier parameterization of the torus containing the signal. The dynamics for the angles that parameterize the torus is the rigid rotation induced by the translation by a vector of basic frequencies of the signal. Unless some prior information on the location of the frequencies is available, the usual way to generate a first approximation to the frequencies is through the discrete Fourier transform (DFT). Specifically, frequencies are approximated by the peaks of the DFT of a sample of points of the signal (see equation (15)). The peak height allows to approximate the amplitude associated with the frequency. The magnitude of the frequency error of this approximation is of $\mathcal{O}(1/N)$, where N is the length of the sample.

The most celebrated method for performing the frequency refinement of the peaks of the DFT was introduced in [10] (see also [11, 12]). Specifically, the quasi-periodic signal is multiplied by suitable window functions (usually a power of the Hanning filter) that considerably improve the resolution of the main peaks of the DFT of the new signal. Once the main frequencies and amplitudes have been determined, their contribution is removed from the original signal. This enhances the resolution of the other frequencies. Further improvements to the DFT techniques include the use of collocation methods (see [6, 7]). By a collocation method we mean trying to fit a finite sample of the signal by a generic quasi-periodic signal defined by a truncated Fourier expansion. This nonlinear system of equations is solved, for both frequencies and amplitudes, by the Newton method. The initial guess of Newton's iteration is that provided by the DFT. We refer the interested reader to the introduction of [15] for further comments and additional references to quasi-periodic frequency analysis.

Another method for the quasi-periodic frequency refinement was introduced in [15]. This method is based on the recursive computation of appropriate weighted sums (that involve the initial iterates or new sequences defined from them), an averaging procedure to normalize these sums and Richardson's extrapolation. We refer to the selected number of recursions performed to define the final recursive sums as the averaging order. Below, we review the main features of [15] together with those of [13, 14, 16, 19], since this collection of papers share a common background. These works tackle the numerical computation of various aspects related to quasi-periodicity in dynamic systems. Among the issues considered, we would like to mention rotation numbers of circle maps [19], frequencies and amplitudes of quasi-periodic signals [15], derivatives of rotation numbers and frequencies with respect to parameters [13], initial conditions of invariant curves of planar maps [14], and initial conditions of Lagrangian invariant tori of Hamiltonian systems and symplectic maps [16]. To accomplish these aims, quasi-periodic signals are dealt with in terms of their frequencies, without simultaneously computing the Fourier representation of any related object (e.g., conjugations to a rigid rotation, invariant curves or invariant tori). Frequencies and their derivatives are computed, in general with remarkable accuracy, by averaging-extrapolation methods applied to a sample of points of the signal (and to the derivatives of the sample when the derivatives of the frequencies come into play). The main requirements of this averaging-extrapolation approach are the analyticity of the signals (although sufficiently large differentiability is enough) and Diophantine vectors of basic frequencies (see definition 2.1 and comments below).

Regarding the frequency refinement, let us suppose kown an approximation $\bar{\omega} \in \mathbb{R}$ to a particular frequency $\omega_0 \in \mathbb{R}$ of a discrete-time quasi-periodic signal $\{x_m\}_{m\in\mathbb{Z}}$ (sometimes a rough approximation may suffice). Then, the method of [15] provides a refined approximation to ω_0. Computations are performed with independence of the contribution to $\{x_m\}_{m\in\mathbb{Z}}$ of the other frequencies and without simultaneously computing the Fourier coefficient associated to ω_0. The method is designed for complex valued signals, but it works as well for real valued ones. The first step to carry out the refinement is to build a new analytic discrete-time quasi-periodic signal of the complex plane that, by its geometrical implications, is referred to as an unfolded signal. The aims of the construction of the unfolded signal $\{x^u_m\}_{m\in\mathbb{Z}}$ are that it should have the same frequencies as $\{x_m\}_{m\in\mathbb{Z}}$, that it should resembles as closely as possible a signal generated by a rigid rotation of the complex plane, and that its rotation frequency around the origin should be the target frequency ω_0. From the geometric perspective, this process is particularly clear in the case of a single independent frequency, since then $\{x_m\}_{m\in\mathbb{Z}}$ evolves on a planar curve. This curve is deformed by the unfolding so that it resembles a circle as closely as possible (see [14]). Computationally speaking, the definition of x^u_m is performed by means of an averaging-extrapolation process. Actually, each iterate of the unfolded signal turns out to be a weighted combination of a prefixed number L of consecutive phase-shifted iterates of $\{x_m\}_{m\in\mathbb{Z}}$, with the phase-shift depending on $\bar{\omega}$, m and L (see equation (10)). As a result of the unfolding, the modulus of the Fourier coefficient associated with the target frequency is amplified with respect to the coefficients associated with the rest of frequencies. This method works even if the initial curve folds over itself or even if it has some self-intersections (provided that the dynamics on it is quasi-periodic). If the approximate frequency $\bar{\omega}$ is close enough to ω_0, the unfolding process allows to generate a new planar curve (with the same frequency) such that, once expressed in polar coordinates, the distance to the origin is a graph of the angle. Therefore, actually making the unfolded signal a graph over the angle is not mandatory in order to be able to use it to refine ω_0. In [14] we provide some graphical illustrations of this deformation process.

In practice, a properly unfolded signal $\{x^u_m\}_{m\in\mathbb{Z}}$ can be computed if $\bar{\omega}$ is reasonably close to a significant frequency ω_0 of $\{x_m\}_{m\in\mathbb{Z}}$ and L is sufficiently large. By "significant frequency" we mean

that the corresponding amplitude "really contributes" to the Fourier representation of the signal. We note that $\{x_m^u\}_{m\in\mathbb{Z}}$ may be non-quasi-periodic for a set of values of $\bar{\omega}$ of zero Lebesgue measure. This fact has no observable effect on practical applications, as the size of the non-quasi-periodic part is exponentially small (see appendix A for more details). Then, by projecting a properly unfolded signal $\{x_m^u\}_{m\in\mathbb{Z}}$ onto a circle, we generate an analytic quasi-periodic signal $\{x_m^c\}_{m\in\mathbb{Z}}$ of the circle. The rotation frequency of $\{x_m^c\}_{m\in\mathbb{Z}}$ is ω_0 (i.e., $\omega_0/2\pi$ is the rotation number). Actually, the mere definition of the rotation number of a circle map works for computing ω_0 from $\{x_m^c\}_{m\in\mathbb{Z}}$, but with a convergence rate of $\mathcal{O}(1/N)$, where N is the lenght of the sample. This slow convergence is improved using the averaging-extrapolation methodology of [19] for the numerical computation of Diophantine rotation numbers of analytic circle maps. It turns out that the approach of [19] also works to compute the rotation frequency of a quasi-periodic signal of the circle, gives rise to a convergence rate of $\mathcal{O}(1/N^{p+1})$ (p is the selected averaging order). We would like to point out that there are other noteworthy methods that could also be used to improve this convergence speed (see [3, 4, 17, 18]). Indeed, it would be an interesting research topic to discuss how these methods fare when used to perform the unfolding procedure of [15] or if we reformulate the refinement process presented in this paper in terms of them (see algorithm 2.5).

Once a sufficiently accurate approximation of ω_0 has been obtained, averaging-extrapolation methods are also capable of computing the associated Fourier coefficient (see equation (12)). Derivatives of the frequencies (with respect to any parameter) can be computed as well from the derivatives of the points of the sample (see [13]). This refinement process can be repeated until we have computed, one by one, a set of basic frequencies of the signal. Initial approximations to the frequencies may be given by the context (e.g., in [16] this methodology has been adapted to the computation of initial conditions of Lagrangian tori with a prefixed frequency vector) or by any frequency analysis method based on DFT. It is worth noting that [15] also provides a "refined" version of the DFT which in the numerical examples of section 4 is used to remove some spurious oscillations around the main peaks of the DFT of a sample of the signal (see algorithm 2.7).

The methodology of [15] has shown good performance in many examples. This is mainly true if a large sample of the signal, computed with sufficiently high numerical accuracy, is known. Perhaps the main drawbacks concern the unfolding process, which must be carried out separately for each frequency to be refined. Selecting averaging order two for the unfolding works quite well in general, but the usual situation is that we do not have any a priori information on what an appropriate value for L would be. Many times, after finding out that the unfolding fails for the selected L, we are forced to restart the unfolding process with a largest L. Therefore, to try to avoid this problem, we sometimes end up generating each unfolded iterate in terms of a significantly larger value of L than is actually required. Although the computational cost of x_m^u is not strongly affected by the value of L (due to the strong correlations between x_m^u and x_{m+1}^u), it can be a matter of concern if N is not very large. Also, after finding out that the unfolding fails, even for very large values of L, we sometimes realize that the approximation $\bar{\omega}$ to ω_0 is not good enough for the unfolding to work.

In this document, we revisit [15] and introduce a new averaging-extrapolation approach to the quasi-periodic frequency refinement that completely avoids the unfolding process. Let $\{x_m\}_{m=1}^{N+1}$ be a known sample of $\{x_m\}_{m\in\mathbb{Z}}$. In algorithm 2.5 we show that $\mathrm{e}^{\mathrm{i}\,\omega_0} \approx x_2^u/x_1^u$, where each complex expression x_1^u and x_2^u is defined by the same process that generates a single iteration of an unfolded signal. Both, x_1^u and x_2^u, are computed using the approximation $\bar{\omega}$, a given averaging order p, and $L = N$ consecutive iterates of the sample. Specifically, we use the sample $\{x_m\}_{m=1}^{N}$ to compute x_1^u and the sample $\{x_{m+1}\}_{m=1}^{N}$ to compute x_2^u. However, unlike what is suggested for a mere unfolding process, here we do not restrict the

averaging order to $p = 2$. In fact, the natural approach would be to consider higher averaging orders. If $\bar{\omega}^{(1)}$ is the new approximation to ω_0 provided by the quotient x_2^u/x_1^u, then we expect the error $|\bar{\omega}^{(1)} - \omega_0|$ to be of the same order of magnitude than the error for the new approximation to ω_0 obtained after performing the full methodology of [15]. The practical implementation of the presented method is quite simple and its computational cost fairly moderate. Hence, it is natural to apply it iteratively to $\bar{\omega}$ until we reach the maximum possible accuracy for ω_0 that we can get from the available sample $\{x_m\}_{m=1}^{N+1}$. Once this iteration is completed, the last computed value of x_1^u directly provides an approximation to the Fourier coefficient associated with ω_0.

2 The method

Below, we summarize the main aspects of the presented methodology. We start by introducing basic notations, definitions and hypotheses. The algorithmic details of the method are formalized in algorithms 2.5, 2.7 and 2.8, but the most technical issues are postponed until appendix A. Some numerical examples are discussed in sections 3 and 4.

Definition 2.1. *A bi-infinite sequence $\{x_m\}_{m\in\mathbb{Z}}$ is a real valued discrete-time quasi-periodic signal if $x_m = \gamma(m\omega)$, where $\omega \in \mathbb{R}^r$ is a frequency vector of the signal, for some r, and $\gamma : \mathbb{T}^r \to \mathbb{R}$ is a function defined on the standard r-dimensional torus $\mathbb{T}^r = (\mathbb{R}/2\pi\mathbb{Z})^r$. If we expand γ in Fourier series,*

$$\gamma(\theta) = \sum_{k\in\mathbb{Z}^r} \hat{\gamma}_k \mathrm{e}^{\mathrm{i}\langle k,\theta\rangle}, \qquad \hat{\gamma}_k = \frac{1}{(2\pi)^r} \int_{\mathbb{T}^r} \gamma(\theta)\, \mathrm{e}^{-\mathrm{i}\langle k,\theta\rangle} d\theta,$$

where $\langle\cdot,\cdot\rangle$ denotes the inner product of $\mathbb{R}^r$, then we have the relation

$$x_m = \gamma(m\omega) = \sum_{k\in\mathbb{Z}^r} \hat{\gamma}_k\, \mathrm{e}^{\mathrm{i}m\langle k,\omega\rangle}, \qquad \forall m \in \mathbb{Z}.$$

The zero Fourier harmonic $\hat{\gamma}_0$ is referred to as the average of the signal.

Definition 2.1 naturally extends to vector valued signals and matrix valued signals, as well as to the case of complex entries. The complete set of frequencies of $\{x_m\}_{m\in\mathbb{Z}}$ is $\{\langle k,\omega\rangle + 2\pi l \,:\, k \in \mathbb{Z}^r,\, l \in \mathbb{Z}\}$, although frequencies that differ by multiples of 2π are equivalent. The components of the vector ω are said to be (rationally) independent if $\langle k,\omega\rangle + 2\pi l \neq 0$, $\forall k \in \mathbb{Z}^r \setminus \{0\}$ and $\forall l \in \mathbb{Z}$. Dependent frequencies mean that the expression $x_m = \gamma(m\omega)$ can be substituted by an equivalent one depending on a smaller number of frequencies. If the components of ω are independent, then they constitute a set of basic frequencies of the signal. If $\omega, \bar{\omega} \in \mathbb{R}^r$ are two different vectors of basic frequencies of $\{x_m\}_{m\in\mathbb{Z}}$, then we have that $\bar{\omega} = \mathcal{M}\omega + 2\pi l$, where $\mathcal{M} \in \mathbb{M}_{r,r}(\mathbb{Z})$ is an unimodular matrix and $l \in \mathbb{Z}^r$. Since we are concerned with Diophantine vectors of frequencies, we assume that there are constants $C > 0$ and $\tau \geq r$ such that

$$|\mathrm{e}^{\mathrm{i}\langle k,\omega\rangle} - 1| \geq C|k|_1^{-\tau}, \qquad \forall k \in \mathbb{Z}^r \setminus \{0\}, \tag{1}$$

where $|k|_1 = |k_1| + \cdots + |k_r|$. This strong nonresonance condition is equivalent to $|\langle k,\omega\rangle + 2\pi l| \geq C'|k|_1^{-\tau}$, $\forall k \in \mathbb{Z}^r \setminus \{0\}$ and $\forall l \in \mathbb{Z}$, for some $C' > 0$.

Although the methods of the paper are also valid for finitely differentiable signals, for the sake of simplicity we restrict the presentation to the analytic case. For further comments on the performance

of averaging-extrapolation methods for the frequency refinement under finite differentiability, we refer the reader to [13, 14, 15, 16, 19]. Essentially, the maximum extrapolation order is then constrained by the differentiability order of γ and the exponent τ of (1). Analyticity of $\{x_m\}_{m\in\mathbb{Z}}$ means that there are constants $\rho > 0$ and $M > 0$ such that

$$|\hat{\gamma}_k| \leq M\mathrm{e}^{-\rho|k|_1}, \quad \forall k \in \mathbb{Z}^r. \tag{2}$$

The lower bound (1) for the small divisors associated with ω, together with the upper bound (2) for the Fourier coefficients of γ, are basic to justify the validity of our approach for any extrapolation order.

Next, we introduce the extrapolation operator that synthesizes the complete averaging-extrapolation process of the paper.

Definition 2.2. *Given positive integers p and $1 \leq N_1 < N_2 < \cdots < N_p = N$, we introduce the operator $\Theta^p_{\{N_j\}} = \Theta^p_{\{N_j\}_{j=1}^p}$, to which we refer to as an extrapolation operator of order p. This operator acts on any finite sequence $\{x_m\}_{m=1}^N$ of length N (real valued, complex valued, vector valued) and is defined by the expression:*

$$\Theta^p_{\{N_j\}}(\{x_m\}_{m=1}^N) = \sum_{l=1}^{p} c_l^p\, \widetilde{S}^p_{N_l},$$

where averaged sums $\widetilde{S}^p_n = \widetilde{S}^p_n(\{x_m\}_{m=1}^N)$ and extrapolation coefficients $c_l^p = c_l^p(\{N_j\}_{j=1}^p)$ are outlined below.

- *The recursive sums $S^l_n = S^l_n(\{x_m\}_{m=1}^N)$, for $n = 1, \ldots, N$, and $l = 0, \ldots, p$, are introduced through the recurrences defined by the following pseudo-code:*

  for $n = 1, \ldots, N$: $S^0_n = x_n$; *end n-loop* ;
  for $l = 0, \ldots, p-1$: $S^{l+1}_1 = S^l_1$;
  for $n = 2, \ldots, N$: $S^{l+1}_n = S^{l+1}_{n-1} + S^l_n$; *end n-loop* ;
  end l-loop ;
- *The averaged sums are $\widetilde{S}^p_n = p!\, S^p_n/n^p$ (we only need them when $n = N_l$, for some $l = 1, \cdots, p$).*
- *The extrapolation coefficients are defined by the following formula:*

$$c_l^p = \prod_{\substack{s=1,\ldots,p \\ s\neq l}} \frac{N_l}{N_l - N_s}, \quad l = 1, \ldots, p. \tag{3}$$

To extrapolate using $\Theta^p_{\{N_j\}}$, it is naural to select integers $\{N_j\}_{j=1}^p$ that behave geometrically with j. Explicitly, we mean that there is $0 < \mu < 1$ such that

$$N_p = N, \quad N_j = [\mu N_{j+1}], \qquad \forall j = p-1, \cdots, 1, \tag{4}$$

where $[x]$ is the function defined as the nearest integer of $x \in \mathbb{R}$. The simplest case is when $\mu = 1/2$ and $N = 2^p M$, for some M. Then, the extrapolation coefficients are independent of M and given by:

$$c_l^p = (-1)^{p-l} \frac{2^{(l-1)l/2}}{\delta(l-1)\delta(p-l)}, \qquad \delta(0) = 1, \quad \delta(s) = (2^s - 1)(2^{s-1} - 1)\cdots(2^1 - 1). \tag{5}$$

Remark 2.3. *For further discussions, from now on we assume that $\{x_m\}_{m=1}^{N+1}$ is a known sample of a real analytic quasi-periodic signal $\{x_m\}_{m\in\mathbb{Z}}$, with a Diophantine frequency vector $\omega \in \mathbb{R}^r$ (see definition 2.1, equation* (1) *and equation* (2)*). We also suppose that, for a prefixed averaging order p, the selected integers $\{N_j\}_{j=1}^{p}$ behave geometrically for some μ, with $N_p = N$ (see equation* (4)*). We denote as $\omega_0 = \langle k_0, \omega\rangle$ a particular frequency of the signal, for some $k_0 \in \mathbb{Z}^r$, and we denote as $\bar{\omega} \approx \omega_0$ a known approximation to ω_0, so that $\varepsilon = |\bar{\omega} - \omega_0|$ verifies $\varepsilon \ll 1$.*

We expect $\Theta^p_{\{N_j\}}(\{x_m\}_{m=1}^N)$ to provide an accurate approximation to the average of $\{x_m\}_{m\in\mathbb{Z}}$. Explicitly, the following asymptotic behaviour is fulfilled as $N \to +\infty$ (see appendix A for details):

$$\Theta^p_{\{N_j\}}(\{x_m\}_{m=1}^N) = \hat{\gamma}_0 + \mathcal{O}(N^{-p}). \tag{6}$$

The main drawback of the approximation $\hat{\gamma}_0 \approx \Theta^p_{\{N_j\}}(\{x_m\}_{m=1}^N)$ is that the expression $\mathcal{O}(N^{-p})$ above involves some terms in which the small divisors associated with ω appear, with exponent p, as denominators of the Fourier coefficients of γ. Therefore, a small C in (1) can yield a large asymptotic coefficient for this error term. It may also be possible that we face a slow convergence speed if the size of some Fourier coefficients $\hat{\gamma}_k$, with $k \neq 0$, is not "small" relative to $\hat{\gamma}_0$. Mainly if the small divisors associated with some of these values of k are significantly small.

If the frequency $\omega_0 = \langle k_0, \omega\rangle$ is known, then it is straightforward to adapt formula (6) to approximate the Fourier coefficient of γ associated to ω_0:

$$\Theta^p_{\{N_j\}}(\{x_m \mathrm{e}^{-\mathrm{i}m\omega_0}\}_{m=1}^N) = \hat{\gamma}_{k_0} + \mathcal{O}(N^{-p}). \tag{7}$$

In applications, the values $\mathrm{e}^{\mathrm{i}m\omega_0}$ can be computed efficiently by trigonometric recurrences. When using formula (7) to address the numerical computation of $\hat{\gamma}_{k_0}$, for increasing values of $|k_0|_1$, we should be aware that $|\hat{\gamma}_{k_0}|$ decreases exponentially fast with $|k_0|_1$ (see comments following algorithm 2.5).

Within the framework of remark 2.3, formula (8) below and its implications are the cornerstone of averaging-extrapolation methods for quasi-periodic frequency refinement. Details are given in appendix A (see equations (28) and (29) and related computations). Explicitly, we have

$$\Theta^p_{\{N_j\}}(\{x_m \mathrm{e}^{-\mathrm{i}m\bar{\omega}}\}_{m=1}^N) = \hat{\gamma}_{k_0}\widetilde{\Delta}_{\{N_j\}}(\mathrm{e}^{\mathrm{i}(\omega_0-\bar{\omega})}) + \widetilde{E}, \tag{8}$$

where $\lim_{\bar{\omega}\to\omega_0} \widetilde{\Delta}_{\{N_j\}}(\mathrm{e}^{\mathrm{i}(\omega_0-\bar{\omega})}) = 1$ and the error term $\widetilde{E}$ satisfies the bound

$$|\widetilde{E}| \leq \frac{\widetilde{C}_1}{C^p}\frac{1}{N^p} + \frac{\widetilde{C}_2}{\exp\left(\widetilde{c}_1/\varepsilon^{1/\tau}\right)}, \tag{9}$$

for some positive constants $\widetilde{C}_1$, $\widetilde{C}_2$ and $\widetilde{c}_1$ that only depend on r, τ, p, M, ρ, $|k_0|_1$, and μ. It is worth mentioning that the expression $\widetilde{\Delta}_{\{N_j\}}(\mathrm{e}^{\mathrm{i}(\omega_0-\bar{\omega})})$ only depends on p, $\{N_j\}_{j=1}^p$, and $\omega_0 - \bar{\omega}$, but it is independent on the specific values of the entries of the sample $\{x_m\}_{m=1}^N$.

If $\bar{\omega} = \omega_0$ and $N \to +\infty$, then the limit value of $\Theta^p_{\{N_j\}}(\{x_m \mathrm{e}^{-\mathrm{i}m\bar{\omega}}\}_{m=1}^N)$ is the Fourier coefficient $\hat{\gamma}_{k_0}$ (compare with (7)). If $\varepsilon = |\bar{\omega} - \omega_0|$ verifies $0 < \varepsilon \ll 1$ and the extrapolation parameters p and $\{N_j\}_{j=1}^p$ are appropriately chosen, we expect $\Theta^p_{\{N_j\}}(\{x_m \mathrm{e}^{-\mathrm{i}m\bar{\omega}}\}_{m=1}^N)$ to be close to $\hat{\gamma}_{k_0}$. By properly chosen, we first mean that a reasonably large N is necessary to actually approach to $\hat{\gamma}_{k_0}$. But it may not be a good idea to take N too large, as it is natural to think that the limit value of $\Theta^p_{\{N_j\}}(\{x_m \mathrm{e}^{-\mathrm{i}m\bar{\omega}}\}_{m=1}^N)$ is zero (this is, indeed, the actual value of the "Fourier coefficient" of $\bar{\omega}$ is it is not a true frequency of the signal).

Formula (8) provides theoretical support to the unfolding procedure introduced in [15]. We proceed by selecting an averaging order $p^u \geq 1$ for the unfolding ($p^u = 2$ works fairly well in general), a (moderately) large positive integer L, and integer values $\{L_j\}_{j=1}^{p_u}$ behaving geometrically as those in equation (4), with $L_{p_u} = L$. The unfolded signal $\{x_n^u\}_{n\in\mathbb{Z}}$ of $\{x_m\}_{m\in\mathbb{Z}}$, computed in terms of the approximate frequency $\bar{\omega}$, is defined by

$$x_n^u = \mathrm{e}^{\mathrm{i}n\bar{\omega}}\,\Theta^{p_u}_{\{L_j\}}(\{x_{n+m-1}\mathrm{e}^{-\mathrm{i}(n+m-1)\bar{\omega}}\}_{m=1}^{L}). \tag{10}$$

If the sample $\{x_m\}_{m=1}^{N}$ is known, for some $N \gg L$, then we can compute the sample $\{x_m^u\}_{m=1}^{N-L+1}$. For almost all values of $\bar{\omega} \approx \omega_0$, the signal $\{x_n^u\}_{n\in\mathbb{Z}}$ turns out to be a complex analytic quasi-periodic signal with the same frequencies as $\{x_m\}_{m\in\mathbb{Z}}$. This assertion may fail for a zero Lebesgue measure set of $\bar{\omega}$. However, from the perspective of applications, we do not have to pay attention to this fact, as we have an exponentially small bound for the non-quasi-periodic contribution (see equation (9)).

Suppose for a moment that we were able to set $\bar{\omega} = \omega_0$. Then, the limit signal of the unfolding, when $L \to \infty$, is the rigid rotation $x_n^u = \hat{\gamma}_{k_0}\mathrm{e}^{\mathrm{i}n\omega_0}$. This means that $x_n^c = \arg(x_n^u) = n\omega_0$ is a quasi-periodic signal of $\mathbb{T}$ with rotation frequency ω_0. Here, the values of the complex argument $\arg(x_n^u)$ are selected according to the rotational dynamics of $\{x_n^u\}_{n\in\mathbb{Z}}$. The idea of [15] is that if $\bar{\omega}$ is close enough to ω_0 and a properly unfolded signal has been computed, then ω_0 becomes the rotation frequency around the origin of $\{x_n^u\}_{n\in\mathbb{Z}}$. In this case, if we are capable of computing the correct determination of $x_n^c = \arg(x_n^u)$, according to the dynamics of $\{x_n^u\}_{n\in\mathbb{Z}}$ in the plane, then it takes the form $x_n^c = n\omega_0 + \phi(n\omega)$. Here, $\phi : \mathbb{T}^r \to \mathbb{C}$ turns out to be an analytic function for which no other specific property is required. This means that the computed signal $\{x_n^c\}_{n\in\mathbb{Z}}$ provides the values of a lift to $\mathbb{R}$ of the signal defined by the projection of $\{x_n^u\}_{n\in\mathbb{Z}}$ onto $\mathbb{T}$. In particular, we can get $\omega_0 = \lim_{n\to+\infty} x_n^c/n$, with a convergence rate of $\mathcal{O}(1/n)$. But, as discussed in the introduction, the application of the methodology of [19] to the sample $\{x_m^c\}_{m=1}^{N-L+1}$ allows to improve this rate up to $\mathcal{O}(1/N^{p_r+1})$. Here, p_r is the selected averaging order for the frequency refinement (it is natural to select it as high as possible).

The following result constitutes the theoretical support to our modified averaging-extrapolation methodology for the quasi-periodic frequency refinement, which we introduce in algorithm 2.5 below.

Proposition 2.4. *With notations, definitions and hypotheses above (see definition 2.1, definition 2.2 and remark 2.3). Let us suppose that the Fourier coefficient associated with $\omega_0 = \langle k_0, \omega\rangle$ verifies $\hat{\gamma}_{k_0} \neq 0$. If $\bar{\omega}$ is sufficiently close to ω_0, then the quotient below provides an improved approximation $\bar{\omega}^{(1)}$ to ω_0:*

$$\mathrm{e}^{\mathrm{i}\bar{\omega}^{(1)}} = \Theta^{p}_{\{N_j\}}(\{x_{m+1}\mathrm{e}^{-\mathrm{i}m\bar{\omega}}\}_{m=1}^{N})/\Theta^{p}_{\{N_j\}}(\{x_m\mathrm{e}^{-\mathrm{i}m\bar{\omega}}\}_{m=1}^{N}). \tag{11}$$

The first crucial point to justify proposition 2.4 is the above mentioned fact that the expression $\widetilde{\Delta}_{\{N_j\}}(\mathrm{e}^{\mathrm{i}(\omega_0-\bar{\omega})})$ of equation (8) does not depend on the sample under consideration. The second crucial point lies in the following observation. Let us assume, according to definition 2.1, that the Fourier representation of the signal $\{x_m\}_{m\in\mathbb{Z}}$ is given by the relation $x_m = \sum_{k\in\mathbb{Z}^r}\hat{\gamma}_k\,\mathrm{e}^{\mathrm{i}m\langle k,\omega\rangle}$. Then, the shifted signal $\{x_{m+1}\}_{m\in\mathbb{Z}}$ verifies $x_{m+1} = \sum_{k\in\mathbb{Z}^r}(\hat{\gamma}_k\,\mathrm{e}^{\mathrm{i}\langle k,\omega\rangle})\,\mathrm{e}^{\mathrm{i}m\langle k,\omega\rangle}$. This means that the quotient between the k-th Fourier coefficients of $\{x_{m+1}\}_{m\in\mathbb{Z}}$ and $\{x_m\}_{m\in\mathbb{Z}}$ equals to $\mathrm{e}^{\mathrm{i}\langle k,\omega\rangle}$.

Algorithm 2.5. *We propose the following construction to carry out the refinement process of a known approximation $\bar{\omega}$ to a frequency ω_0 of a quasi-periodic signal $\{x_m\}_{m\in\mathbb{Z}}$.*

1. *Select an averaging order $p \geq 1$, a geometric ratio $0 < \mu < 1$, and compute a (large) sample of iterates $\{x_m\}_{m=1}^{N+1}$ of the signal so that, if we define the integers $\{N_j\}_{j=1}^{p}$ as in* (4)*, then $N_1 \gg 1$.*

2. *Compute a new approximation $\bar{\omega}^{(1)}$ to $\bar{\omega}$ using equation* (11)*. Explicitly, we use definition 2.2 to compute $\Theta^p_{\{N_j\}}(\{x_{m+1}\mathrm{e}^{-\mathrm{i}m\bar{\omega}}\}_{m=1}^N)$ and $\Theta^p_{\{N_j\}}(\{x_m\mathrm{e}^{-\mathrm{i}m\bar{\omega}}\}_{m=1}^N)$. We define $\bar{\omega}^{(1)}$ as the value of the complex argument of its quotient closest to $\bar{\omega}$.*
3. *Set $\bar{\omega} = \bar{\omega}^{(1)}$ as a new (improved) approximation to ω_0 and apply again the previous step. In this way, we define a sequence $\{\bar{\omega}^{(n)}\}_{n\geq 1}$. A natural way to estimate the iterative error for $\bar{\omega}^{(n)}$ is to compute the difference between two consecutive iterations, i.e., $|\bar{\omega}^{(n)} - \bar{\omega}^{(n-1)}|$. Then, we can increase n until the estimated error does not improve after two consecutive iterations.*
4. *We denote by $\bar{\omega}^* = \bar{\omega}^{(n^*)}$, for some $n^* \geq 1$, the final value thus computed. Since the sequence $\{\bar{\omega}^{(n)}\}_{n\geq 1}$ does not actually converge to ω_0, what we expect is that if ω_0 is a significant enough frequency of the signal, then $|\bar{\omega}^* - \omega_0|$ should be of $\mathcal{O}(1/N^p)$.*
5. *We also can compute the following approximation to the Fourier coefficent associated with ω_0:*

$$\hat{\gamma}_{k_0} \approx \Theta^p_{\{N_j\}}(\{x_m\mathrm{e}^{-\mathrm{i}m\bar{\omega}^*}\}_{m=1}^N). \tag{12}$$

Below, we summarize some issues to consider in the numerical implementation of algorithm 2.5.

- The first step of the process, before the actual application of algorithm 2.5 itself, should be to replace the computed sample $\{x_m\}_{m=1}^{N+1}$ by $\{x_m - \bar{x}\}_{m=1}^{N+1}$, where $\bar{x}$ is a numerical value for the average $\hat{\gamma}_0$ of the signal. This approximation to the average can be computed, with an $\mathcal{O}(N^{-p})$ convergence rate, without knowing any frequency. We just need to use formula (12) with $\bar{\omega}^* = 0$. We note that the substraction of $\bar{x}$ does not result in any error for the frequencies. However, in many cases the average turns out to be the largest Fourier coefficient of the signal and can therefore be an important source of noise for any averaging-extrapolation method. We also observe that, for a given signal $\{x_m\}_{m\in\mathbb{Z}}$, the numerical validation of the fast convergence speed of the average can be used as an indicator that we are really dealing with a quasi-periodic signal (see [3, 4, 16, 17, 18]).
- We recommend to use as large values of p as possible to apply algorithm 2.5. However, we have to be aware that, as we increase p, we need also to increase N in order to really achieve an $\mathcal{O}(1/N^p)$ behaviour for the error. The numerical accuracy of the sample is also a limitation for the efficiency of the method, as many cancellations occur when applying Richardson's extrapolation. The computational cost of each iteration of the refinement process is independent on the number of basic frequencies.
- When performing the sums S_n^l of definition 2.2 numerically, we have to be aware of the fact that $S_n^l = \mathcal{O}(n^l)$ to avoid losing too much numerical precision. To try to overcome this problem, there is the option of a computer arithmetic with a large number of decimal digits. As an alternative, all the numerical computations below have been performed using a computer arithmetic of double precision, while storing separately the integer and decimal parts of the recursive sums S_n^p. Furthermore, before starting the iterative computation of these sums, we recommend to scale all iterates by the maximum of their moduli (this scaling factor should be subsequently removed when necessary).
- Taking $\mu = 1/2$ allows to use explicit formulas (5) for the extrapolation coefficients. Taking also $N = 2^Q$ facilitates the computation of several extrapolated values for $\bar{\omega}^{(1)}$, by dealing simultaneously with several different averaging orders and several samples of different length. In the presented numerical examples, we proceed as follows. We choose a maximum extrapolation order P and, for any p between 1 and P, we compute $\bar{\omega}^{(1)}_{(p,q)}$ as the extrapolated value for $\bar{\omega}^{(1)}$ (provided by formula (11)) obtained by using averaging order p, $\mu = 1/2$, and a sample of length $2^q + 1$. The value of q moves from a minimum value $q_0 \geq P$ to Q. For each fixed p, we estimate the error $e_{(p,q)}$ of $\bar{\omega}^{(1)}_{(p,q)}$ by comparing the

(p,q)-extrapolated value with the $(p,q-1)$-extrapolated one:

$$e_{p,q} = |\bar{\omega}^{(1)}_{(p,q)} - \bar{\omega}^{(1)}_{(p,q-1)}|, \qquad 1 \le p \le P,\ q_0+1 \le q \le Q. \tag{13}$$

We take as a numerical value for $\bar{\omega}^{(1)}$ the value $\bar{\omega}^{(1)}_{(p^*,q^*)}$ that minimizes $e_{p,q}$, i.e.:

$$e_{p^*,q^*} = \min_{1\le p\le P,\, q_0+1\le q\le Q} \{e_{p,q}\}. \tag{14}$$

We will use the same criteria to try to determine which is the "best" extrapolated value (among all those obtained) when computing the average of the signal or any other associated Fourier coefficient.

- We have to be aware that even though the iterative error $|\bar{\omega}^{(n^*)} - \bar{\omega}^{(n^*-1)}|$ of $\bar{\omega}^* = \bar{\omega}^{(n^*)}$ may be very small, it does not mean that we are approaching a true frequency ω_0 of the signal with such precision. The actual accuracy $|\bar{\omega}^* - \omega_0|$ is strongly conditioned by how dominant the Fourier coefficient associated with ω_0 is (with respect to the other Fourier coefficients) and by the proximity to ω_0 of other dominant frequencies in the signal. In particular, if the numerical value of the Fourier coefficient associated with $\bar{\omega}^*$ is significantly small, then this probably means that we have in fact refined a spurious frequency of the signal, perhaps very inaccurately. This aspect is discussed in section 4.
- As previously noted with regard to DFT methods, the removal of the Fourier contribution of the frequencies already computed enhances the visibility of the other ones. But this removal may be not necessary in the framework of averaging-extrapolation methods, since the Fourier contribution of any frequency, other than the target one, is averaged out very fast. Therefore, if we know approximations to a set of basic frequencies of $\{x_m\}_{m\in\mathbb{Z}}$, and all these frequencies have a sufficiently significant amplitude, then we expect to be able to refine each of them by dealing with the initial signal (without performing any removal). Conversely, if we remove the Fourier contribution of the previously refined frequencies, then we are introducing an additional source of error for the other ones.
- Once a complete set of basic frequencies has been refined, we can approach the computation of an accurate as possible Fourier representation of the signal. In this case, we are faced with a different situation from the one discussed above. In order to compute $\hat{\gamma}_{k_0}$ for increasing values of $|k_0|_1$, it may be better to apply formula (12) not to the original signal, but to the signal obtained after removing from $\{x_m\}_{m\in\mathbb{Z}}$ the Fourier contribution associated with the previously computed coefficients. In the numerical examples, we first compute the Fourier coefficients of order 1 (in fact they are already known) by dealing with $\{x_m\}_{m\in\mathbb{Z}}$ minus its average. Next, we remove the Fourier contribution of order 1 from it and compute the Fourier coefficients of ordre 2 from this residual signal. And so on.

To place the peaks on the real line providing the first approximations to the frequencies, we rely of the first order correction of the DFT provided by the unfolding process (see [15]). Precisely, let us consider the sample $\{x_m\}_{m=1}^L$ of the initial quasi-periodic signal, for some moderately large L (although here the same symbol L is being used, the actual value of L has nothing to do with the one used to introduce the unfolding process). The DFT approach consists of searching for the peaks with respect $\bar{\omega}$ of the function

$$Z^1(\bar{\omega}) = \left|\Theta^1_{\{L\}}(\{x_m \mathrm{e}^{-\mathrm{i}m\bar{\omega}}\}_{m=1}^L)\right| = \frac{1}{L}\left|\sum_{m=1}^{L} x_m \mathrm{e}^{-\mathrm{i}m\bar{\omega}}\right|. \tag{15}$$

To try to increase the visibility of the main peaks, we suggest to take L even and to use the function:

$$Z^2(\bar{\omega}) = \left|\Theta^2_{\{L/2,L\}}(\{x_m \mathrm{e}^{-\mathrm{i}m\bar{\omega}}\}_{m=1}^L)\right| = \frac{4}{L^2}\left|S^2_L(\{x_m \mathrm{e}^{-\mathrm{i}m\bar{\omega}}\}_{m=1}^L) - 2\, S^2_{L/2}(\{x_m \mathrm{e}^{-\mathrm{i}m\bar{\omega}}\}_{m=1}^{L/2})\right|. \tag{16}$$

We can ease the computation of $Z^2(\bar{\omega})$ by using the explicit formula $S_L^2(\{x_m\}_{m=1}^L) = \sum_{l=1}^L (L-l+1)\, x_l$. We can adapt definition (16) to define $Z^p(\bar{\omega})$, for any $p > 2$. However, the larger p is, the larger L must be to actually improve the frequency resolution by using $Z^p(\bar{\omega})$. For a large p and a very large L, the main peaks of $Z^p(\bar{\omega})$ become strongly narrowed and any numerical approach faces the risk of omitting some of them. Therefore, we proceed by taking $p = 2$.

Remark 2.6. *If ω is a frequency of a discrete-time quasi-periodic signal, then we can always get an equivalent one in the interval $(-\pi, \pi)$. If the signal has real entries and ω is a frequency, then so is $-\omega$ (the associated Fourier coefficients are one the complex conjugate of the other). Hence, for real signals, it is sufficient to look for (independent) frequencies in the interval $(0, \pi)$.*

Algorithm 2.7. *We propose the following construction to carry out the computation of the first approximations to the dominant frequencies of a real valued quasi-periodic signal $\{x_m\}_{m\in\mathbb{Z}}$ as peaks of Z^2.*

1. *Select a moderately large even value of L and consider the sample $\{x_m\}_{m=1}^L$.*
2. *To avoid having a dominant peak for $\bar{\omega} = 0$, we replace the sample $\{x_m\}_{m=1}^L$ by $\{x_m - \bar{x}\}_{m=1}^L$, where $\bar{x}$ is a numerical value for the average ($\bar{x}$ can be computed using a larger sample).*
3. *Select a moderately large M and consider the sample $\{\bar{\omega}^{(m)}\}_{m=1}^M$ of equispaced values of $\bar{\omega} \in (0, \pi]$.*
4. *Use formula* (16) *to compute the value of Z^2 for the points in this sample, i.e., $\{Z^2(\bar{\omega}^{(m)})\}_{m=1}^M$.*
5. *We compute the first approximations to the dominant frequencies as those defining the main peaks of $\{Z^2(\bar{\omega}^{(m)})\}_{m=1}^M$. We proceed recursively as follows. The first peak corresponds to the index j_1 such that $Z^2(\bar{\omega}^{(j_1)})$ maximizes Z^2 among the sample. Next, we redefine Z^2 by setting $Z^2(\bar{\omega}^{(j)}) = 0$ for those j belonging to the "support" of this peak, i.e., for those j with $\hat{J}_1 \leq j \leq \widetilde{J}_2$, in such a way the value of $Z^2(\bar{\omega}^{(j)})$ increases with j if $\hat{J}_1 \leq j \leq j_1$, and decreases with j if $j_1 \leq j \leq \widetilde{J}_2$. The second peak corresponds to the index j_2 such that $Z^2(\bar{\omega}^{(j_2)})$ maximizes the new function Z^2 thus defined. And so on, until the desired number of peaks is obtained.*
6. *Before applying to them algorithm 2.5, there is the chance to improve these peaks by refining the sample of values of Z^2 around them.*

Once the approximations to frequencies of $\{x_m\}_{m\in\mathbb{Z}}$ provided by algorithm 2.7 have been refined through algorithm 2.5, we are then faced with the issue of deciding which of these refined frequencies are independent and which are a combination of the others. This process can be computationally expensive if the signal has a large number of independent frequencies (as is the case in section 4.2). To carry out it numerically, we introduce the following definition. Given a vector $\omega \in \mathbb{R}^r$ and an integer $M \geq 1$, we introduce the quantity:

$$\varepsilon^{(M)}(\omega) = \min\left\{ \left| \left\langle k, \frac{\omega}{2\pi} \right\rangle - m \right| \,:\, k \in \mathbb{Z}^r,\, 0 < |k|_1 \leq M,\, m \in \mathbb{Z} \right\}, \tag{17}$$

i.e., $\varepsilon^{(M)}(\omega)$ stands for the strongest quasi-resonance verified, up to order M, by the components of ω.

Algorithm 2.8. *We propose the following construction to analyze resonances between a set of refined frequencies $\{\omega_{\text{ref}}^{(j)}\}_{j=1}^R$ of a quasi-periodic signal.*

1. *Sort the entries of $\{\omega_{\text{ref}}^{(j)}\}_{j=1}^R$ in decreasing order according to the numerical value of the modulus of the associated Fourier coefficient (i.e., from most dominant to least dominant). Frequencies with a significantly small Fourier coefficient should be eliminated from the discussion.*

2. *Select a moderately large integer $N_R \geq 1$ and a small tolerance $\varepsilon_R > 0$ (of size comparable to the actual accuracy with which we know the refined frequencies). We will assume that the components of a frequency vector ω are (numerically) rationally dependent if $\varepsilon^{(M)}(\omega) < \varepsilon_R$.*
3. *We first compute $\varepsilon^{(N_R)}(\omega^{(1)}_{\rm ref}, \omega^{(2)}_{\rm ref})$. If $\omega^{(1)}_{\rm ref}$ and $\omega^{(2)}_{\rm ref}$ are found to be "independent", then we compute $\varepsilon^{(N_R)}(\omega^{(1)}_{\rm ref}, \omega^{(2)}_{\rm ref}, \omega^{(3)}_{\rm ref})$. And so on until some set of frequencies becomes "resonant".*
4. *When we detect that a certain set of frequencies verifies a resonant relation, we remove from the set the less dominant one for which the coefficient of the integer combination defining this resonance is ± 1. If none of the coefficient is equal to ± 1, then we report the resonance, but we do not remove any frequency (we have not faced this situation in any numerical example). We then add the next frequency in the list to the set and proceed again. And so on, until we have extracted a set of independent frequencies among those in $\{\omega^{(j)}_{\rm ref}\}_{j=1}^{R}$.*

Remark 2.9. *Instead of the definition $\mathbb{T} = \mathbb{R}/2\pi\mathbb{Z}$ used in the presentation above, for the numerical examples in sections 3 and 4 we set $\mathbb{T} = \mathbb{R}/\mathbb{Z}$. This means that, instead of dealing with a quasi-periodic signal in terms of its frequencies, we are dealing with the corresponding rotation frequencies. We do this only to simplify the handling of resonances between frequencies, which is one of the main aspects of section 4. Therefore, this modification does not affect the implementation details of the methods at all. We only have to be aware of the fact that the considered Fourier expansions must be of the form*

$$\gamma(\theta) = \sum_{k \in \mathbb{Z}^r} \hat{\gamma}_k \mathrm{e}^{2\pi \mathrm{i} \langle k, \theta \rangle} \tag{18}$$

and that in all the formulas involving any frequency ω, we must replace it by $2\pi\widetilde{\omega}$, where $\widetilde{\omega}$ is the associated rotation frequency.

3 Numerical example for an explicit signal

In this section, we discuss the numerical performance of the presented methodology by dealing with a quasi-periodic signal $\{x_m\}_{m\in\mathbb{Z}}$ defined by an explicit formula. Given a vector of rotation frequencies $\widetilde{\omega} \in \mathbb{R}^r$ and $\nu = \mathrm{e}^{2\pi\,\rho}$, for some $\rho > 0$, we define:

$$x_m = \gamma(n\,\widetilde{\omega}), \quad m \in \mathbb{Z}, \qquad \gamma(\theta) = 2\,\mathrm{Re}\left(\prod_{j=1}^{r} \frac{1}{1 - \nu\,\mathrm{e}^{2\pi\mathrm{i}\theta_j}}\right), \quad \theta \in \mathbb{T}^r = (\mathbb{R}/\mathbb{Z})^r. \tag{19}$$

The Fourier coefficients of γ (see (18)) are all zero apart from its average $\hat{\gamma}_0 = 2$ and $\hat{\gamma}_k = \nu^{|k|_1}$, for those $k \in \mathbb{Z}^r \setminus \{0\}$ for which $k_j \geq 0$, $\forall j = 1, \ldots, r$, or for which $k_j \leq 0$, $\forall j = 1, \ldots, r$. Furthermore, the maximum possible value for the width of the strip of analyticity of γ around $\mathbb{T}^r$ equals to ρ, which allows us to illustrate the significance of the size of this width in the good performance of our approach.

We present results for $r = 5$ and for $r = 10$. For $r = 10$ we select the following rotation vector $\widetilde{\omega} \in \mathbb{R}^{10}$ for the quasi-periodic forcing (whose components belong to $(0, 1/2)$):

$$(\sqrt{2}-1, 2-\sqrt{3}, \sqrt{5}-2, 3-\sqrt{7}, \sqrt{11}-3, 4-\sqrt{13}, \sqrt{17}-4, \sqrt{19}-4, 5-\sqrt{23}, \sqrt{29}-5). \tag{20}$$

For $r = 5$, we select $\widetilde{\omega} \in \mathbb{R}^5$ as the one defined by the 5 first components of (20). Some outstanding quasi-resonances, up to order 10, for the selected rotation frequencies $\widetilde{\omega} \in \mathbb{R}^5$ are $\varepsilon^{(3)} \approx 1.2 \cdot 10^{-3}$,

$\varepsilon^{(5)} \approx 2.9 \cdot 10^{-4}$ and $\varepsilon^{(9)} \approx 5.1 \cdot 10^{-5}$, where $\varepsilon^{(M)} = \varepsilon^{(M)}(2\pi\widetilde{\omega})$ (see equation (17)). The same analysis for $r = 10$ results in $\varepsilon^{(2)} \approx 4.7{\cdot}10^{-3}$, $\varepsilon^{(3)} \approx 2.7{\cdot}10^{-4}$, $\varepsilon^{(4)} \approx 1.8{\cdot}10^{-5}$, $\varepsilon^{(6)} \approx 1.5{\cdot}10^{-6}$, $\varepsilon^{(9)} \approx 5.1{\cdot}10^{-8}$.

Our plan is to fix not only $r \in \{5, 10\}$ and $\widetilde{\omega} \in \mathbb{R}^r$, but also to fix the value of all the parameters involved in the implementation of algorithms 2.5 and 2.7. This uniformity on the numerical computations allows us to visualize the behaviour of the different methods for decreasing values of ρ. Hence, once we set a particular ρ, we first compute an approximate value $\bar{x}_r(\rho)$ for the average of (19). Since the true value of the average is know, we can evaluate the actual error $|\bar{x}_r(\rho) - 2|$. In addition, we can also use formulas (13) and (14) to compute the corresponding estimated error for $\bar{x}_r(\rho)$. We denote as $\mathrm{L}_r(\rho)$ and $\mathrm{l}_r(\rho)$ the $\log_{10}$ of the actual error and the estimated error, respectively. We compute the $\log_{10}$ of the errors since it provides minus the number of correct decimal digits. The next step is to directly select the r peaks of $Z^2(2\pi\omega)$ (computed as a function of the rotation frequency $\omega \in (0, 0.5]$) that are closest to each of the components of $\widetilde{\omega}$. We then try to refine each of these peaks by means of algorithm 2.5 and compute the actual error of each of the final refined values. The function $\mathrm{R}_r(\rho)$ accounts for the $\log_{10}$ of the maximum of the errors of these r refined peaks. However, as ρ decreases, the graph of Z^2 becomes so wild that it is not possible to locate adequate approximations to the components of $\widetilde{\omega}$ from its peaks, unless we drastically improve the computational parameters of Z^2. This is clearly apparent in the top left plot of figure 1, where we display $Z^2(2\pi\omega)$ for $r = 10$ and $\rho = 0.09$ (the graph of $Z^1(2\pi\omega)$ is quite similar). This is because for small ρ there is a significant amount of γ Fourier harmonics in (19) with an amplitude very similar to those associated to the $\widetilde{\omega}$ components. Then, when we find out that for a small ρ we are unable to use Z^2 to detect approximations to all the components of $\widetilde{\omega}$, we do not deal with this ρ and neither do we deal with smaller values of ρ. Let us note that this stopping criterion does not mean that algorithm 2.5 is not capable of refining the significant peaks of Z^2 to signal rotation frequencies (although the final accuracy may decrease drastically with ρ). For the values of ρ for which we have been able to refine all the components of $\widetilde{\omega}$, we also compute the Fourier coefficients of the signal associated with integer combinations, up to a prefixed order, of the set of basic rotation frequencies $\widetilde{\omega}$. To carry out these computations, we have taken into account the last of the issues discussed following algorithm 2.5. As the value of all the Fourier coefficients of γ is known, we can compute the actual error of each of them. Since Fourier coefficients go to zero as the order increases, it makes sense to deal not with their absolute error, but with their relative error. Indeed, we have divided the absolute error of each coefficient of order k by ν^k (the same normalization is also applied to the absolute error of those coefficients of order k that we know must be zero). For a fixed r, we denote by $\mathrm{F}_k(\rho)$ the $\log_{10}$ of the maximum of these relative errors, computed among the Fourier coefficients of a given order $k \geq 1$.

The chosen parameters for the implementation of the case $r = 5$ are the following. We consider 47 equispaced values of $\rho \in [0.04, 0.5]$, with step 0.01. Therefore, $\nu = \mathrm{e}^{-2\pi\rho}$ moves between 0.0432 and 0.7778. For $\rho = 0.03$ we have not been able to use the computed sample of the function Z^2 to locate approximations of all the components of $\widetilde{\omega}$. For each value of ρ within the selected range, we have computed the sample $\{x_m\}_{m=1}^{N+1}$ of the quasi-periodic signal (19), with $N = 2^{20}$. All the averaging-extrapolation processes carried out in connection with algorithm 2.5 (i.e., frequency refinement and computation of the average and of other Fourier coefficients) have been performed as discussed in connection with equations (13) and (14), by using extrapolation orders p between 1 and $P = 10$, and samples of length 2^q, with q ranging from $q_0 = 10$ and $Q = 20$. To approximate the frequencies by the peaks of $Z^2(2\pi\omega)$, we have considered the sample $\{\widetilde{\omega}^{(j)}\}_{j=1}^{10000}$ of equispaced values of the rotation frequency $\omega \in (0, 1/2]$, while we have used $L = 2^{12}$ to evaluate $Z^2(2\pi\widetilde{\omega}^{(j)})$ through formula (16). Next, we have computed the 15 dominant peaks of the sample $\{Z^2(2\pi\widetilde{\omega}^{(j)})\}_{j=1}^{10000}$, and we have identified which

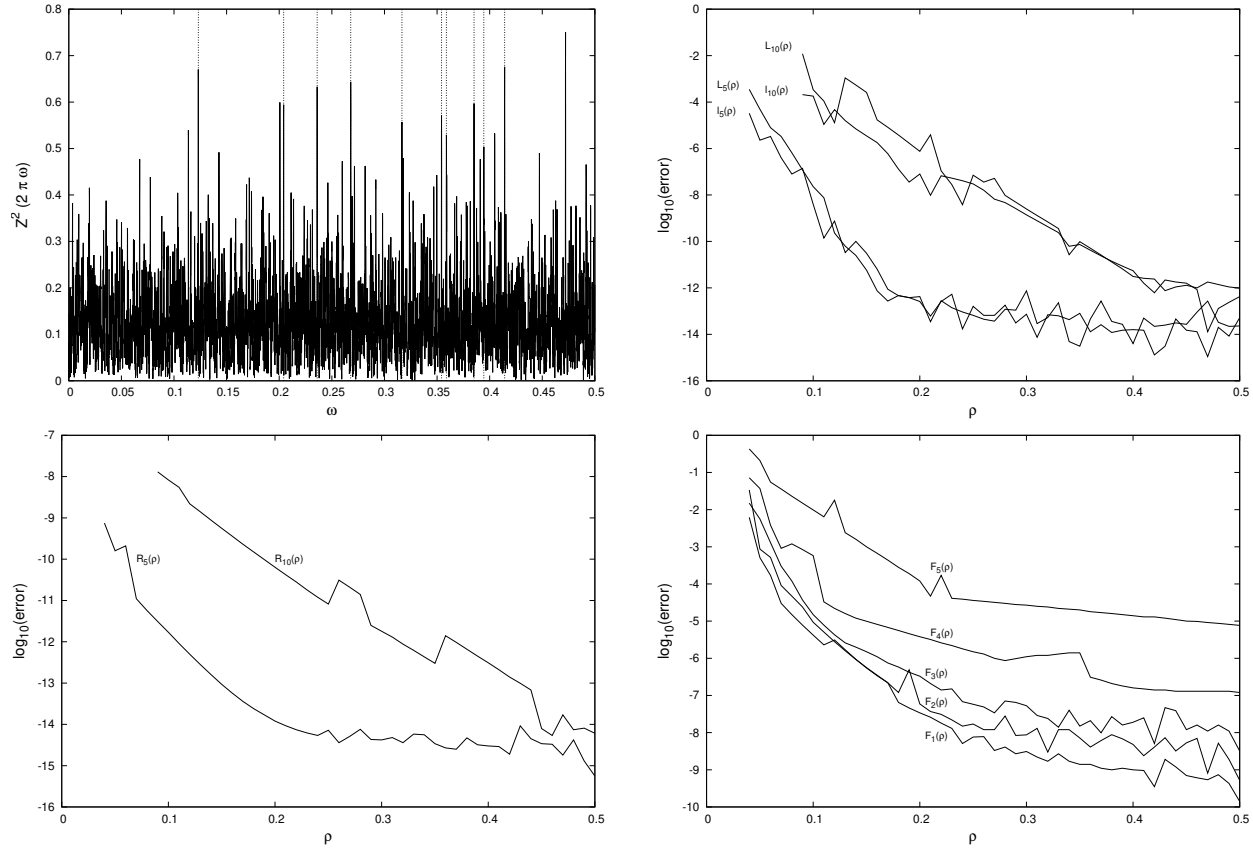

Figure 1: Graphs for results on signal (19). Top left: $Z^2(2\pi\omega)$ vs. ω for $r = 10$, $\rho = 0.09$. Top right: $\log_{10}$ of the estimated error and the actual error, for $r = 5$ and $r = 10$, of the computed average vs. ρ. Bottom left: $\log_{10}$ of the maximum of the actual errors, for $r = 5$ and $r = 10$, of the refined rotation frequencies vs. ρ. Bottom right: $\log_{10}$ of the maximum, for $r = 5$, of the actual relative errors of the refined Fourier coefficients of orders from 1 to 5 vs. ρ.

of them is really close to each of the components of $\widetilde{\omega} \in \mathbb{R}^5$. To carry out the frequency refinement of each selected peak of Z^2, we have performed 6 iterations of the refinement method of algorithm 2.5. After 4 iterations we have, in general, reached the highest possible accuracy for any of them (similar behaviour occurs with the other frequency refinement processes im the paper). Finally, approximation to the Fourier coefficients of the signal have been computed, for each selected ρ, up to order 5. For $r = 5$, the total number of complex Fourier coefficients up to order 5 is 1683, although we do not compute those which are the complex conjugate of one already calculated. We proceed similarly for $r = 10$, but now we can deal with 42 equispaced values of $\rho \in [0.09, 0.5]$, with step 0.01 ($\nu = \mathrm{e}^{-2\pi\rho}$ moves between 0.0432 and 0.5681). To approximate the components of $\widetilde{\omega} \in \mathbb{R}^{10}$ for each of these ρ, we have identified the 30 first peaks of Z^2 associated to a sample of 15000 equispaced values of the rotation frequency in $(0, 1/2]$. The frequency refinement of each of the selected 10 peaks has been performed in the same way as for $r = 5$. Finally, Fourier coefficients up to order 4 have been computed (for $r = 10$ the total number of complex Fourier coefficients up to order 5 is 8361).

In table 1 we show the 4 first iterations of the refinement of the computed peak of Z^2 closest to $\widetilde{\omega}_1$. Left table corresponds to $r = 5$ and $\rho = 0.04$ and right table to $r = 10$ and $\rho = 0.09$. Columns labelled

ω	err_ω	Err_ω	ω	err_ω	Err_ω
0.414200000000000		$1.4 \cdot 10^{-5}$	0.414200000000000		$1.4 \cdot 10^{-5}$
0.414213600063258	$1.4 \cdot 10^{-5}$	$3.8 \cdot 10^{-8}$	0.414215075053919	$1.5 \cdot 10^{-5}$	$1.5 \cdot 10^{-6}$
0.414213561586767	$3.8 \cdot 10^{-8}$	$7.9 \cdot 10^{-10}$	0.414213610516040	$1.5 \cdot 10^{-6}$	$4.8 \cdot 10^{-8}$
0.414213563754556	$2.2 \cdot 10^{-9}$	$1.4 \cdot 10^{-9}$	0.414213562381056	$4.8 \cdot 10^{-8}$	$8.0 \cdot 10^{-12}$
0.414213561624734	$2.1 \cdot 10^{-9}$	$7.5 \cdot 10^{-10}$	0.414213562075675	$3.1 \cdot 10^{-10}$	$3.0 \cdot 10^{-10}$

Table 1: Iterative results of the refinement of the peak of $Z^{(2)}(2\pi\omega)$ closest to $\widetilde{\omega}_1$ for the signal (19). Left table corresponds to $r = 5$ and $\rho = 0.04$. Right table corresponds to $r = 10$ and $\rho = 0.09$.

as ω give the sequence of values of the rotation frequency, while e_ω and E_ω are the iterative error and the actual error, respectively. Iterative errors are defined from the difference between the values before and after iteration (so they are not defined for the first row). In addition to the aforementioned graph of $Z^2(2\pi\omega)$ for $r = 10$ and $\rho = 0.09$ (upper left plot), in figure 1 we display some graphs showing the behaviour of the errors in the computation of the average, frequencies and Fourier coefficients as ρ decreases. The top right plot shows the $\log_{10}$-errors functions $\mathrm{L}_r(\rho)$ and $\mathrm{l}_r(\rho)$ introduced above from the errors on the computation of the average of the signal, for $r \in \{5, 10\}$. It is worth mentioning that the actual and estimated errors in the computation of the average behave quite similarly (as is also the case in the frequency refinement of the components of $\widetilde{\omega}$). The bottom left plot displays the $\log_{10}$-error function $\mathrm{R}_r(\rho)$ associated to the maximum of the actual errors on the refined frequencies, for $r \in \{5, 10\}$. The bottom left plot shows the $\log_{10}$-error functions $\mathrm{F}_k(\rho)$, associated to the maximum of the relative errors on the Fourier coefficients of order $k = 1, \ldots, 5$, but only for $r = 5$. We do not show the corresponding $\log_{10}$-error functions for $r = 10$ because they only provide significant results for $k \in \{1, 2\}$. For $k > 2$, the relative errors in the Fourier coefficients become of order one if ρ is small, probably because in this case there are a very large amount of Fourier coefficients of very similar size to those of order one.

4 Numerical example for a quasi-periodically forced standard map

The second example to show the numerical performance of the methodology is the quasi-periodically forced Chirikov's standard map $F_{\alpha,\beta,\widetilde{\omega}} : (\widetilde{\theta}, x, y) \in \mathbb{T}^r \times \mathbb{T} \times \mathbb{R} \to (\widetilde{\theta}', x', y') \in \mathbb{T}^r \times \mathbb{T} \times \mathbb{R}$, defined as:

$$\widetilde{\theta}' = \widetilde{\theta} + \widetilde{\omega}, \qquad y' = y + \alpha \sin(2\pi x) + \beta \sum_{j=1}^{r} \sin(2\pi \widetilde{\theta}_j), \qquad x' = x + y'. \tag{21}$$

The map (21) defines a quasi-periodic analytic skew-product of $\mathbb{T} \times \mathbb{R}$, with rotation frequencies $\widetilde{\omega} \in \mathbb{R}^r$. We suppose that the corresponding vector of frequencies, given by $2\pi\widetilde{\omega}$, verifies a Diophantine condition (see (1)). Enlarging the phase space to $\mathbb{T}^r \times \mathbb{T} \times \mathbb{R}^r \times \mathbb{R}$, by the addition of appropriate new variables $\widetilde{I} \in \mathbb{R}^r$, allows to rewrite (21) as an exact symplectic map for the actions $(\widetilde{\theta}, x)$ and the momenta $(\widetilde{I}, y)$ (these new variables $\widetilde{I}$ do not mean any modification for the dynamics of $(\widetilde{\theta}, x, y)$). Since for $\alpha = \beta = 0$ the map (21) is an integrable and non-degenerate twist map, then we expect to have plently of KAM (primary) invariant tori of $F_{\alpha,\beta,\widetilde{\omega}}$ if $0 < |\alpha|, |\beta| \ll 1$. These tori carry quasi-periodic motion with a rotation vector of the form $\omega = (\widetilde{\omega}, \hat{\omega}) \in \mathbb{R}^r \times \mathbb{R}$. The inner rotation frequency $\hat{\omega}$ should be close to the value of the y coordinate along the torus.

We have selected the map (21) for several reasons. From its iterates we can generate non-trivial quasi-periodic signals, which are not defined *ad hoc*. The computational cost of each iteration is relatively mild, since the expression $\sum_{j=1}^{r}\sin(2\pi\widetilde{\theta}_j)$ can be evaluated recursively by trigonometric recurrences. Moreover, if we iterate the map for a large set of initial conditions, all with the same initial value for $\widetilde{\theta}$, then the sequence of iterates of this trigonometric sum is the same for all these points. Finally, before starting the frequency analysis, we have strong control for the $r+1$ frequencies of each quasi-periodic solution that belongs to a primary invariant torus. Indeed, not only the frequencies of the forcing are known a priori, but the average of the discrete-time signal defined by the component y of the iterates gives the value of the inner rotation frequency $\hat{\omega}$. Explicitly, let $(x,y)=\varphi(\theta)$ be a parameterization of an $(r+1)$-dimensional invariant torus of $F_{\alpha,\beta,\widetilde{\omega}}$, in such a way that the dyamics for $\theta=(\widetilde{\theta},\hat{\theta})\in\mathbb{T}^r\times\mathbb{T}$ is a rigid rotation of rotation vector $\omega=(\widetilde{\omega},\hat{\omega})$. This means that the functional (invariance) equation $F_{\alpha,\beta,\widetilde{\omega}}(\widetilde{\theta},\varphi(\theta))=(\widetilde{\theta}+\widetilde{\omega},\varphi(\theta+\omega))$ holds. If φ parametrizes a primary torus of the map, then we can express $(x,y)=\varphi(\theta)$ as $x=\hat{\theta}+\phi(\theta)$ and $y=\psi(\theta)$, with $\phi(\theta)$ and $\psi(\theta)$ 1-periodic on the angles (i.e., the torus in the (x,y) space is homotopic to $\mathbb{T}\times\{0\}$). Consequently, this invariance equation reads as:

$$\psi(\theta+\omega)=\psi(\theta)+\alpha\sin(2\pi\,(\hat{\theta}+\phi(\theta)))+\beta\sum_{j=1}^{r}\sin(2\pi\widetilde{\theta}_j),\quad \hat{\omega}+\phi(\theta+\omega)=\phi(\theta)+\psi(\theta+\omega).$$

In particular, expressions above mean that the average with respect to θ of $\psi(\theta)$ equals to $\hat{\omega}$.

We consider initial conditions of the form $(\widetilde{\theta}^{(1)},x^{(1)},y^{(1)})=(0,0,y_0)$, with $0\leq y_0\leq 1$, and perform the iteration $(\widetilde{\theta}^{(m+1)},x^{(m+1)},y^{(m+1)})=F_{\alpha,\beta,\widetilde{\omega}}(\widetilde{\theta}^{(m)},x^{(m)},y^{(m)})$, $m\geq 1$. If an initial condition belongs to a primary invariant torus of $F_{\alpha,\beta,\widetilde{\omega}}$, then $\{y^{(m)}\}_{m\geq 1}$ defines a quasi-periodic signal with rotation vector $\omega=(\widetilde{\omega},\hat{\omega})$, whose average is $\hat{\omega}$. We then first try to numerically compute the average $\hat{\gamma}_0$ of $\{y^{(m)}\}_{m\geq 1}$ from a sample of the signal. As noted in the introduction, if $\hat{\gamma}_0$ can be computed with significantly large accuracy, then we can use this fact as a first indicator that this time-discrete signal is quasi-periodic. Therefore, in order to really expect that we have a primary torus, we also have to check that the computed value $\hat{\omega}=\hat{\gamma}_0$ (the candidate to inner rotation frequency of the torus) is non-resonant with the rotation vector $\widetilde{\omega}$ of the forcing. A resonance between $\hat{\omega}$ and $\widetilde{\omega}$ may mean that the initial condition belongs to a non-primary invariant torus contained in a resonant zone of the map. From the numerical viewpoint, non-resonance means $\varepsilon^{(N_R)}(2\pi\widetilde{\omega},2\pi\hat{\omega})>\varepsilon_R$, for some $N_R\gg 1$ and $0<\varepsilon_R\ll 1$ (see algorithm 2.8).

We present results for $r=5$ and for $r=10$ by using the same rotation vectors $\widetilde{\omega}\in\mathbb{R}^r$ introduced in section 3. Hence, the selected ε_R above should be in consonance with $\varepsilon^{(N_R)}(2\pi\widetilde{\omega})$ (see equation (20) and related comments). Furthermore, to reduce the amount of parameters, we set $\alpha=0.01$ fixed throughout the computations. This α is clearly below the critical value $\alpha_{GM}\approx 0.971635/2\pi\approx 0.15464$ corresponding to the breakdown of the last invariant curve of the Chirikov's standard map (with rotation frequency the Golden Mean).

4.1 Results for $r=5$

We perform a numerical exploration to detect candidates for initial conditions $(\widetilde{\theta}^{(1)},x^{(1)},y^{(1)})=(0,0,y_0)$ giving rise to primary invariant tori of $F_{0.01,\beta,\widetilde{\omega}}$. We consider 101 equispaced values of $\beta\in[0,0.02]$ and, for each of these β, we consider 1001 initial conditions defined by equispaced values of $y_0\in[0,1]$. After iteration of each initial condition, we use the y-coordinate to generate the sample $\{y^{(m)}(y_0,\beta)\}_{m=1}^{N+1}$, with

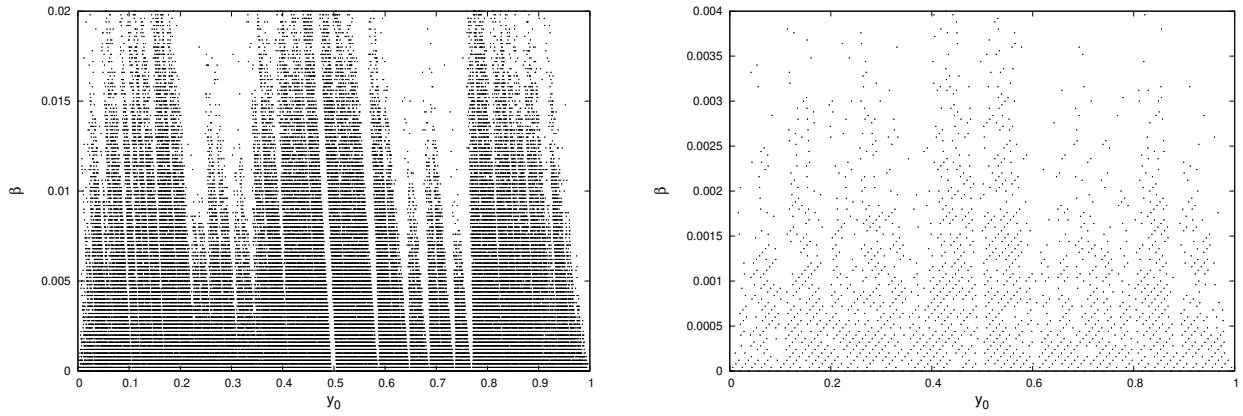

Figure 2: Couples (y_0, β) for which we expect that the selected initial conditions (numerically) define a primary invariant torus of the map $F_{0.01,\beta,\widetilde{\omega}}$ for $r = 5$ (left plot) and $r = 10$ (right plot).

$N = 2^{20}$. We proceed as described in comments following algorithm 2.5 in order to compute a numerical value $\hat{\omega}(y_0, \beta)$ for the average of $\{y^{(m)}(y_0, \beta)\}_{m\geq 1}$ as well as an estimated error $e(y_0, \beta)$. Explicitly, we rely on the methodology discussed in connection with equations (13) and (14), using extrapolation orders p between 1 and $P = 6$, and samples of length 2^q, with q ranging from $q_0 = 10$ and $Q = 20$. The same implementation has been used below to evaluate each averaging-extrapolation operator associated to the frequency refinement and to the computation of the Fourier coefficients, as well as to estimate the associated errors. We first purge the selected collection of parameters (y_0, β) by removing those for which $e(y_0, \beta)$ is larger than 10^{-9}. Next, we remove those parameters for which $\hat{\omega} = \hat{\omega}(y_0, \beta)$ does not verify $\varepsilon^{(N_R)}(2\pi\widetilde{\omega}, 2\pi\hat{\omega}) > \varepsilon_R$ for $N_R = 10$ and $\varepsilon_R = 10^{-7}$. The couples (y_0, β) and (y_0', β') for which $|\hat{\omega}(y_0, \beta) - \hat{\omega}(y_0', \beta')| < 10^{-7}$ are also removed. We do so because if two values of the inner frequency are so close, for different parameters, it seems reasonable to think that they are associated with a (higher order) resonance. The surviving values of (y_0, β) (about 41% of the initial ones) are displayed in the left plot of figure 2. For these values we expect that $\{y^{(m)}(y_0, \beta)\}_{m\geq 1}$ numerically behaves as a true quasi-periodic signal, with vector of rotation frequencies given by $(\widetilde{\omega}, \hat{\omega})$, with $\hat{\omega} \approx \hat{\omega}(y_0, \beta)$.

Among the surviving parameters, we focus on $\beta = 0.014$ and $y_0 = 0.82$ (so we can omit the dependence on (y_0, β) until the end of this sub-section). This is the analysed pair (y_0, β) which gives rise to an estimated error of order 10^{-11} (or smaller) for as large as possible β. For the associated discretre signal $\{y^{(m)}\}_{m\geq 1}$, we get the values $\hat{\omega} = \hat{\omega}_{3,18} \approx 0.83397589718242415$ and $e \approx 1.5 \cdot 10^{-11}$ (we observe that $\hat{\omega}$ is reasonably close to y_0). For this particular case, we have repeated the computation of the average by allowing averaging order up to $p = 10$. We get the new (improved) values $\hat{\omega} = \hat{\omega}_{10,17} \approx 0.83397589848930753$ and $e \approx 7.8 \cdot 10^{-13}$. The smaller quasi-resonance obtained up to ordrer 12 for this computed value for $\hat{\omega}$ is $\varepsilon^{(12)}(2\pi\widetilde{\omega}, 2\pi\hat{\omega}) \approx 1.1 \cdot 10^{-6}$ (see equation (17)).

The first step in performing the frequency refinement on $\{y^{(m)}\}_{n\geq 1}$ is to obtain initial approximations to the frequencies. We proceed as if we had no prior information on any of them. We introduce the signal $\{x_m\}_{m\geq 1}$ by removing from $y^{(m)}$ the estimated value for its average, i.e., $x_m = y^{(m)} - \hat{\omega}$. We then use the sample $\{x_m\}_{m=1}^{L}$, with $L = 2^{12}$, to compute the modulus Z^1 of the DFT and the modulus Z^2 of the "refined" DFT transform (see equations (15) and (16)). In the upper part of figure 3 we display $Z^1(2\pi\omega)$ (left plot) and $Z^2(2\pi\omega)$ (right plot) after computing both for 1000 equispaced values of the rotation frequency $\omega \in (0, 0.5]$. We observe that the dominant peaks of Z^2 are narrower than those of Z^1

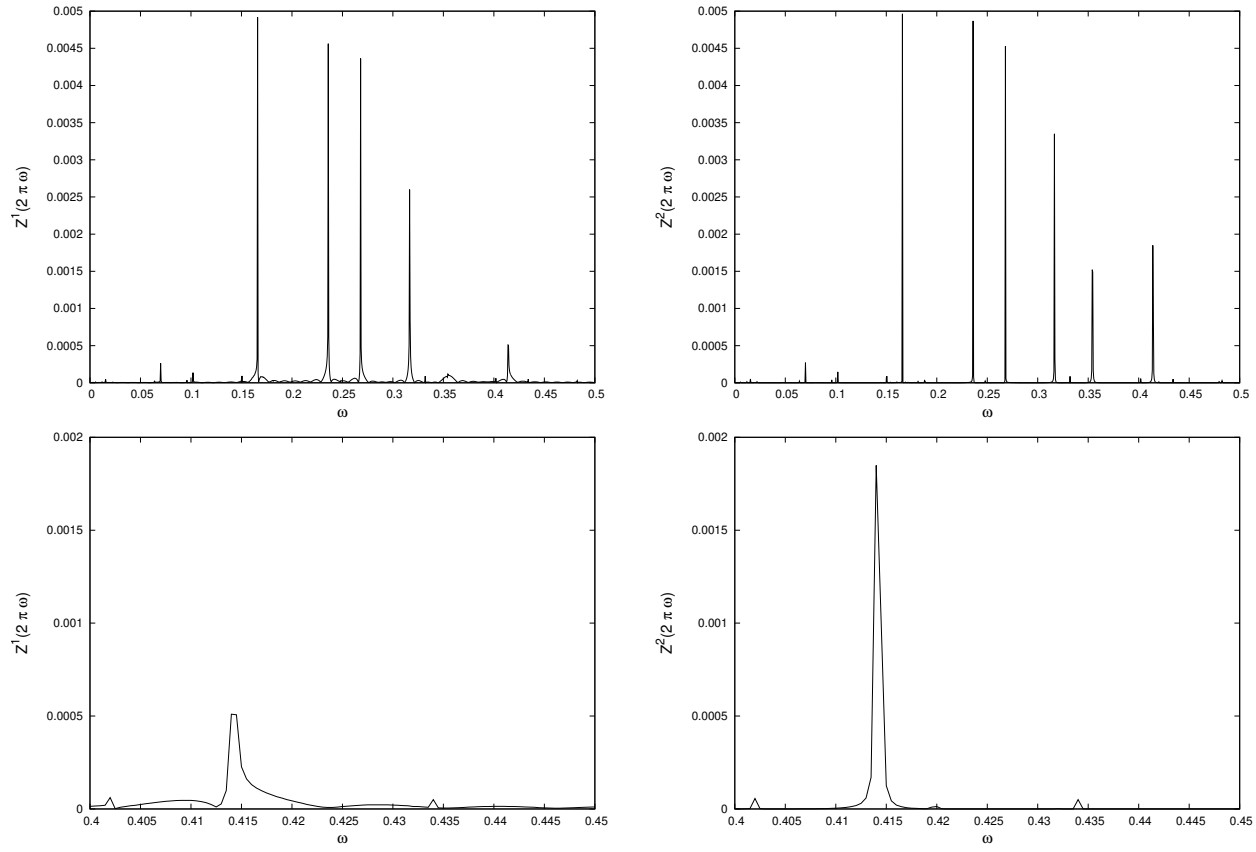

Figure 3: Graphs of $Z^1(2\pi\omega)$ (left) and of $Z^2(2\pi\omega)$ (right) for the selected signal generated by the y-coordinate of $F_{\alpha,\beta,\widetilde{\omega}}$ for $r = 5$.

and that some spurious oscillations have been eliminated. This is mainly visible in the zoomed-in lower graphs. We then have tried to obtain approximations to rotation frequencies of $\{y^{(m)}\}_{n\geq 1}$ from the 15 first peaks of the above computed sample $\{Z^2(2\pi\omega^{(j)})\}_{j=1}^{1000}$ (see algorith 2.7). These peakes have been iteratively refined (along with associated Fourier coefficients) using algorithm 2.5. We have performed 6 iterations of the refinement method for each approximate frequency but, in fact, after 4 iterations we have reached the highest possible accuracy for any of them. In table 2, we show the first 4 iterations for two of the approximate frequencies. The two columns labelled by ω give the iterates of the rotation frequency, while err_ω and $\mathrm{err}_{\mathrm{coef}_\omega}$ give the iterative errors for ω and for the Fourier coefficient coef_ω, respectively. Since $1.66 \approx 1 - \hat{\omega}$ (see remark 2.6), where $\hat{\omega}$ is the previously computed value for the average of $\{y^{(m)}\}_{m\geq 1}$, we expect that the sequence of values in the first column approaches to a value close to the inner frequency $1 - \hat{\omega}$ of the signal (see comments below).

A summary of the results for all refined frequencies is shown in table 3, where rotation frequencies are sorted in decreasing order according to the modulus of the Fourier coefficient $\mathrm{coef}_{\omega_{\mathrm{ref}}}$ associated with the refined frequency ω_{ref}. As we are not removing from the signal the Fourier contribution of previously refined frequencies, the selected refinement order is not important. In table 3, ω_{peak} is the initial approximation to the frequency provided by a peak of Z^2. Further, $\mathrm{err}_{\omega_{\mathrm{ref}}}$ and $\mathrm{err}_{\mathrm{coef}_{\omega_{\mathrm{ref}}}}$ are the the errors of the refinement method for ω_{ref} and $\mathrm{coef}_{\omega_{\mathrm{ref}}}$, respectively. Refinement errors are defined

ω	err_{ω}	$\mathrm{err}_{\mathrm{coef}_{\omega}}$	ω	err_{ω}	$\mathrm{err}_{\mathrm{coef}_{\omega}}$
0.166000000000000			0.07000000000000000		
0.166024094641940	$2.4 \cdot 10^{-5}$	$5.1 \cdot 10^{-3}$	0.07004387216647549	$4.4 \cdot 10^{-5}$	$3.6 \cdot 10^{-4}$
0.166024101510722	$6.9 \cdot 10^{-9}$	$5.1 \cdot 10^{-6}$	0.07004387468195829	$2.5 \cdot 10^{-9}$	$5.0 \cdot 10^{-7}$
0.166024101510723	$1.1 \cdot 10^{-15}$	$8.4 \cdot 10^{-13}$	0.07004387468195822	$6.9 \cdot 10^{-17}$	$1.6 \cdot 10^{-14}$
0.166024101510725	$1.3 \cdot 10^{-15}$	$1.0 \cdot 10^{-12}$	0.07004387468195820	$1.4 \cdot 10^{-17}$	$3.5 \cdot 10^{-15}$

Table 2: Iterative results of the refinement for two of the peaks for the selected signal generated by the y-coordinate of $F_{\alpha,\beta,\widetilde{\omega}}$ for $r = 5$.

using the difference between the two last iterates. We recall that $\mathrm{err}_{\omega_{\mathrm{ref}}}$ does not necessary reflects the accuracy of ω_{ref} as a frequency of the signal. Hence, we have also computed, when possible, the error $\mathrm{Err}_{\omega_{\mathrm{ref}}}$ defined by comparing ω_{ref} with the corresponding true rotation frequency of the quasi-periodic forcing (rows 1, 3 to 6) or with the previously computed value $1-\hat{\omega}$ for the inner frequency of $\{y^{(m)}\}_{m\geq 1}$ (row 2). Errors of the frequency refinement for these 6 frequencies match quite well with those expected.

Since the number of independent frequencies is not set a priori when applying the method, the next step is to numerically detect resonances (up to order 10) between refined frequencies. We have not examined $\omega_{\mathrm{ref}}^{(15)}$, as its Fourier coefficient is extremly small. Peaks of Z^2 giving rise to a refined frequency with a very small amplitude should come from spurious peaks (probably related to oscillations due to "secondary" frequencies contained in the peak's support of a "dominant" frequency). Not omitting these frequencies a priori has the problem that they may be related to high order resonances that can be difficult to detect, as these frequencies are probably known with a low level of accuracy. We have used the methodology proposed in algorithm 2.8 to analyze resonances between $\{\omega_{\mathrm{ref}}^{(j)}\}_{j=1}^{14}$. As a conclussion, we confirm that $\{\omega_{\mathrm{ref}}^{(j)}\}_{j=1}^{6}$ are independent, and we derive the following relations for the remaining ones:

$$\omega_{\mathrm{ref}}^{(7)} \approx \omega_{\mathrm{ref}}^{(1)} - \omega_{\mathrm{ref}}^{(2)}, \quad \omega_{\mathrm{ref}}^{(8)} \approx \omega_{\mathrm{ref}}^{(3)} - \omega_{\mathrm{ref}}^{(2)}, \quad \omega_{\mathrm{ref}}^{(9)} \approx \omega_{\mathrm{ref}}^{(4)} - \omega_{\mathrm{ref}}^{(2)}, \quad \omega_{\mathrm{ref}}^{(10)} \approx 2\,\omega_{\mathrm{ref}}^{(2)},$$
$$\omega_{\mathrm{ref}}^{(11)} \approx \omega_{\mathrm{ref}}^{(5)} - \omega_{\mathrm{ref}}^{(2)}, \quad \omega_{\mathrm{ref}}^{(12)} \approx \omega_{\mathrm{ref}}^{(1)} + \omega_{\mathrm{ref}}^{(2)}, \quad \omega_{\mathrm{ref}}^{(13)} \approx \omega_{\mathrm{ref}}^{(2)} + \omega_{\mathrm{ref}}^{(3)}, \quad \omega_{\mathrm{ref}}^{(14)} \approx 2\,\omega_{\mathrm{ref}}^{(2)} - \omega_{\mathrm{ref}}^{(1)}.$$

These relations are used to define $\mathrm{Err}_{\omega_{\mathrm{ref}}}^{(j)}$ for $j = 7, \ldots, 14$ in table 3. E.g., $\mathrm{Err}_{\omega_{\mathrm{ref}}}^{(7)} = |\omega_{\mathrm{ref}}^{(7)} - \omega_{\mathrm{ref}}^{(1)} + \omega_{\mathrm{ref}}^{(2)}|$.

We have also computed the Fourier coefficients of the quasi-periodic signal $\{y^{(m)}\}_{m\geq 1}$ associated with integer combinations, up to order 5, of the set of basic rotation frequencies $\{\omega_{\mathrm{ref}}^{(j)}\}_{j=1}^{6}$. Harmonics of order 6 are so small that it is unrealistic to expect any significant accuracy for them. The total number of complex Fourier coefficients up to order 5, for 6 frequencies, is 3653. To compute the Fourier coefficients we have used the approach suggested in the comments that follow algorithm 2.5. Therefore, we first compute the Fourier coefficients of order 1 (in fact they are already known) by dealing with the signal $\{y^{(m)}\}_{m\geq 1}$ minus its average. Next, we remove the Fourier contribution of order 1 from $\{y^{(m)}\}_{m\geq 1}$ and compute the Fourier coefficients of ordre 2 from this residual signal. And so on. We denote by $m^{(n)}$, for $n \geq 0$, the maximum size of the modulus of the iterates $\{y^{(m)}\}_{m=1}^{N}$ after the removal of their Fourier harmonics up to order n. We have obtained $m^{(0)} = 5.4 \cdot 10^{-2}$, $m^{(1)} = 2.0 \cdot 10^{-3}$, $m^{(2)} = 5.3 \cdot 10^{-4}$, $m^{(3)} = 2.7 \cdot 10^{-4}$, $m^{(4)} = 2.0 \cdot 10^{-4}$, and $m^{(5)} = 1.7 \cdot 10^{-4}$. Although $m^{(n)}$ does not decrease too fast with n, this fact has not been an obstacle to compute fairly good approximations for the frequencies. We point out that we have generally observed that the numerical results of averaging-extrapolation methods for frequencies are usually better than those for the Fourier coefficients (which, in fact, is very common in all frequency analysis methods).

j	$\omega_{\text{peak}}^{(j)}$	$\omega_{\text{ref}}^{(j)}$	$\text{err}_{\omega_{\text{ref}}}^{(j)}$	$\lvert\text{coef}_{\omega_{\text{ref}}}^{(j)}\rvert$	$\text{err}_{\text{coef}_{\omega_{\text{ref}}}}^{(j)}$	$\text{Err}_{\omega_{\text{ref}}}^{(j)}$
1	0.2360	0.236067977499787	$7.5 \cdot 10^{-16}$	$5.2 \cdot 10^{-3}$	$5.7 \cdot 10^{-12}$	$2.6 \cdot 10^{-15}$
2	0.1660	0.166024101510724	$4.4 \cdot 10^{-15}$	$5.0 \cdot 10^{-3}$	$2.6 \cdot 10^{-12}$	$3.1 \cdot 10^{-14}$
3	0.2680	0.267949192431126	$4.7 \cdot 10^{-15}$	$4.7 \cdot 10^{-3}$	$4.5 \cdot 10^{-12}$	$3.1 \cdot 10^{-15}$
4	0.3165	0.316624790355398	$3.4 \cdot 10^{-15}$	$4.2 \cdot 10^{-3}$	$1.6 \cdot 10^{-11}$	$2.2 \cdot 10^{-15}$
5	0.3540	0.354248688935411	$3.6 \cdot 10^{-15}$	$3.9 \cdot 10^{-3}$	$2.2 \cdot 10^{-11}$	$1.2 \cdot 10^{-15}$
6	0.4140	0.414213562373096	$2.8 \cdot 10^{-15}$	$3.6 \cdot 10^{-3}$	$4.6 \cdot 10^{-11}$	$8.3 \cdot 10^{-16}$
7	0.0700	0.070043874681958	$1.4 \cdot 10^{-17}$	$2.8 \cdot 10^{-4}$	$3.5 \cdot 10^{-15}$	$1.3 \cdot 10^{-9}$
8	0.1020	0.101925089613485	$2.8 \cdot 10^{-17}$	$1.6 \cdot 10^{-4}$	$4.5 \cdot 10^{-15}$	$1.3 \cdot 10^{-9}$
9	0.1505	0.150600687655115	$3.4 \cdot 10^{-15}$	$1.1 \cdot 10^{-4}$	$6.7 \cdot 10^{-14}$	$1.9 \cdot 10^{-9}$
10	0.3320	0.332048203021388	$7.9 \cdot 10^{-15}$	$9.1 \cdot 10^{-5}$	$7.1 \cdot 10^{-14}$	$3.1 \cdot 10^{-15}$
11	0.1880	0.188224586235124	$1.0 \cdot 10^{-15}$	$6.7 \cdot 10^{-5}$	$5.8 \cdot 10^{-14}$	$1.2 \cdot 10^{-9}$
12	0.4020	0.402092079010574	$4.1 \cdot 10^{-15}$	$6.4 \cdot 10^{-5}$	$2.7 \cdot 10^{-14}$	$9.2 \cdot 10^{-14}$
13	0.4340	0.433973293941802	$1.7 \cdot 10^{-16}$	$5.1 \cdot 10^{-5}$	$2.2 \cdot 10^{-14}$	$1.3 \cdot 10^{-14}$
14	0.0960	0.095980228138780	$1.2 \cdot 10^{-14}$	$4.0 \cdot 10^{-5}$	$3.5 \cdot 10^{-13}$	$2.6 \cdot 10^{-9}$
15	0.0155	0.015499878428198	$2.0 \cdot 10^{-10}$	$5.2 \cdot 10^{-11}$	$5.8 \cdot 10^{-14}$	

Table 3: Results of the refinement process for the selected signal generated by the y-coordinate of $F_{\alpha,\beta,\widetilde{\omega}}$ for $r = 5$.

4.2 Results for $r = 10$

Once again, we set $\alpha = 0.01$ and perform a numerical exploration of the map by computing the average of the y-coordinate. Now, we select a mesh of 1001×101 values for the pair $(y_0, \beta) \in [0, 1] \times [0, 0.004]$ (equispaced in both directions). The numerical value $\hat{\omega}(y_0, \beta)$ for the average of $\{y^{(m)}(y_0, \beta)\}_{m \geq 1}$ and the estimate $e(y_0, \beta)$ for its error are both computed as done for $r = 5$ (using the same number of iterates and the same averaging-extrapolation orders). We have applied the same purge to the set of parameters (y_0, β) as done for $r = 5$, with the only difference that we only check the non-resonance conditions up to order $N_R = 8$. The verification of these non-resonances is by far the most time-consuming part of these computations. In this case, only about 1.7% of these initial points survive (see the right plot of figure 2). We note that, in fact, about 22% of them survive if we only eliminate those for which we have detected a resonance up to order $N_R = 8$. Many other initial conditions have been suppressed because we are assuming that if a pair of different initial conditions give rise to very close values of $\hat{\omega}(y_0, \beta)$ it is because they are probably resonant.

We select $\beta = 0.00392$ and $y_0 = 0.195$ as parameters that we expect to define a primary torus of the map for $r = 10$ (from now on we omit any dependence on (y_0, β)). For this pair (y_0, β) we get the values $\hat{\omega} = \hat{\omega}_{4,19} \approx 0.21793798707514395$ (not "too far" from y_0) and $e \approx 2.4 \cdot 10^{-12}$. The smaller quasi-resonance, up to ordrer $N_R = 8$, between $\hat{\omega}$ and the frequencies of the forcing is $\varepsilon^{(8)}(\widetilde{\omega}, \hat{\omega}) \approx 8.6 \cdot 10^{-7}$ (see equation (17)). We compute the functions $Z^1(2\pi\omega)$ and $Z^2(2\pi\omega)$ for the signal $\{x_m\}_{m \geq 1}$ defined as $x_m = y^{(m)} - \hat{\omega}$, using the same implementation parameters as for $r = 5$. The graphical comparison of the peaks of Z^1 (left graphs) with those of Z^2 (right graphs) is shown in figure 4.

We discuss the results of the refinement process for the 15 "dominant" peaks of the computed sample $\{Z^2(2\pi\omega^{(j)})\}_{j=1}^{1000}$. Refinement has been performed using the same implementation parameters as for $r = 5$. In particular, we have done 6 iterations for every approximate frequency provided by each of

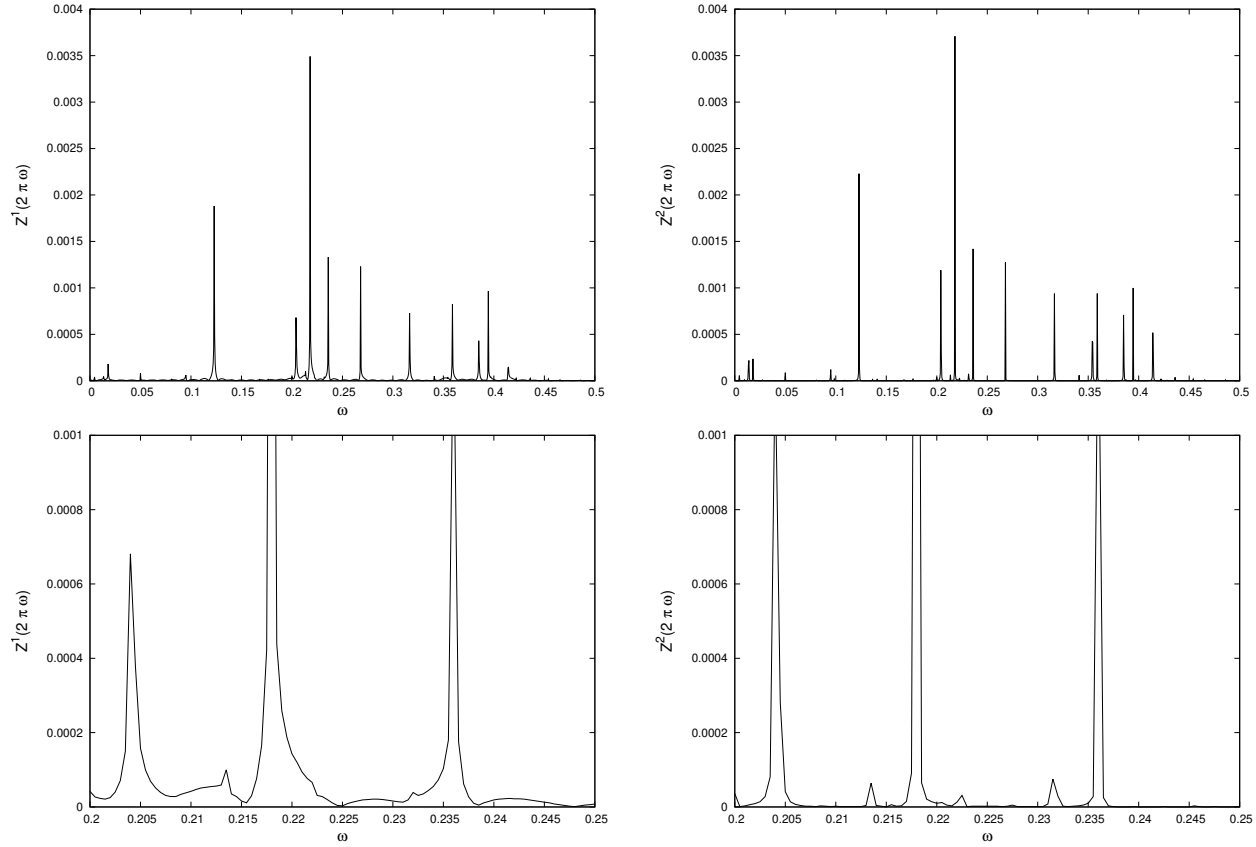

Figure 4: Graphs of $Z^1(2\pi\omega)$ (left) and of $Z^2(2\pi\omega)$ (right) for the selected signal generated by the y-coordinate of $F_{\alpha,\beta,\widetilde{\omega}}$ for $r = 10$.

ω	err_ω	$\mathrm{err}_{\mathrm{coef}_\omega}$	ω	err_ω	$\mathrm{err}_{\mathrm{coef}_\omega}$
0.2180000000000000			0.05000000000000000		
0.2179385328503463	$6.1 \cdot 10^{-5}$	$3.5 \cdot 10^{-3}$	0.05001176875732311	$1.2 \cdot 10^{-5}$	$1.4 \cdot 10^{-4}$
0.2179379935504115	$5.4 \cdot 10^{-7}$	$5.4 \cdot 10^{-3}$	0.05001119810412949	$5.7 \cdot 10^{-7}$	$1.2 \cdot 10^{-4}$
0.2179379947008482	$1.2 \cdot 10^{-9}$	$1.5 \cdot 10^{-5}$	0.05001119779828809	$3.1 \cdot 10^{-10}$	$8.9 \cdot 10^{-8}$
0.2179379947001661	$6.8 \cdot 10^{-13}$	$8.8 \cdot 10^{-9}$	0.05001119779844358	$1.6 \cdot 10^{-13}$	$4.5 \cdot 10^{-11}$
0.2179379947001665	$3.9 \cdot 10^{-16}$	$5.1 \cdot 10^{-12}$	0.05001119779844351	$6.9 \cdot 10^{-17}$	$1.9 \cdot 10^{-14}$

Table 4: Iterative results of the refinement for two of the peaks for the selected signal generated by the y-coordinate of $F_{\alpha,\beta,\widetilde{\omega}}$ for $r = 10$.

these peaks. Table 4 shows the iterative process for two of these approximate frequencies (compare with table 2) and table 5 shows a summary of the results for all these approximations (compare with table 3). Entries in table 3 with error equal to zero are due to the fact that, after some iterations of the refinement process applied to these frequencies, there is no difference between two consecutive values of these quantities (in terms of the used double precision arithmetic). As expected, refinement of the approximations associated with the first 11 peaks yields the internal frequency of the torus and the frequencies of the forcing (the corresponding errors are those in the last column). The difference

j	$\omega^{(j)}_{\text{peak}}$	$\omega^{(j)}_{\text{ref}}$	$\text{err}^{(j)}_{\omega_{\text{ref}}}$	$\lvert\text{coef}^{(j)}_{\omega_{\text{ref}}}\rvert$	$\text{err}^{(j)}_{\text{coef}_{\omega_{\text{ref}}}}$	$\text{Err}^{(j)}_{\omega_{\text{ref}}}$
1	0.2180	0.21793799470016659	$5.6 \cdot 10^{-17}$	$3.9 \cdot 10^{-3}$	$5.1 \cdot 10^{-12}$	$7.6 \cdot 10^{-9}$
2	0.1230	0.12310562561766709	$3.7 \cdot 10^{-16}$	$2.6 \cdot 10^{-3}$	$1.6 \cdot 10^{-12}$	$6.5 \cdot 10^{-15}$
3	0.2040	0.20416847668727622	$1.8 \cdot 10^{-15}$	$1.8 \cdot 10^{-3}$	$9.1 \cdot 10^{-12}$	$4.7 \cdot 10^{-15}$
4	0.2360	0.23606797749977840	$1.4 \cdot 10^{-15}$	$1.5 \cdot 10^{-3}$	$5.2 \cdot 10^{-12}$	$1.1 \cdot 10^{-14}$
5	0.2680	0.26794919243111931	$1.7 \cdot 10^{-16}$	$1.3 \cdot 10^{-3}$	$4.6 \cdot 10^{-13}$	$3.5 \cdot 10^{-15}$
6	0.3165	0.31662479035539526	0	$1.2 \cdot 10^{-3}$	0	$4.6 \cdot 10^{-15}$
7	0.3540	0.35424868893539035	$6.1 \cdot 10^{-15}$	$1.1 \cdot 10^{-3}$	$1.8 \cdot 10^{-11}$	$1.9 \cdot 10^{-14}$
8	0.3590	0.35889894354065921	$5.6 \cdot 10^{-17}$	$1.1 \cdot 10^{-3}$	$5.1 \cdot 10^{-12}$	$1.5 \cdot 10^{-14}$
9	0.3850	0.38516480713450540	$2.0 \cdot 10^{-15}$	$1.0 \cdot 10^{-3}$	$5.1 \cdot 10^{-12}$	$1.7 \cdot 10^{-15}$
10	0.3945	0.39444872453600111	$5.6 \cdot 10^{-17}$	$1.0 \cdot 10^{-3}$	$7.0 \cdot 10^{-12}$	$9.8 \cdot 10^{-15}$
11	0.4140	0.41421356237305801	$3.2 \cdot 10^{-15}$	$1.0 \cdot 10^{-3}$	$1.2 \cdot 10^{-11}$	$3.7 \cdot 10^{-14}$
12	0.0500	0.05001119779844351	0	$8.8 \cdot 10^{-5}$	$1.9 \cdot 10^{-14}$	$6.7 \cdot 10^{-11}$
13	0.0950	0.09500213189842259	$8.3 \cdot 10^{-17}$	$4.5 \cdot 10^{-6}$	$1.2 \cdot 10^{-14}$	$1.2 \cdot 10^{-9}$
14	0.0180	0.01800004701773137	$1.1 \cdot 10^{-7}$	$4.1 \cdot 10^{-8}$	$8.0 \cdot 10^{-8}$	
15	0.0140	0.01399779145758519	$2.6 \cdot 10^{-10}$	$6.9 \cdot 10^{-8}$	$3.2 \cdot 10^{-10}$	

Table 5: Results of the refinement process for the selected signal generated by the y-coordinate of $F_{\alpha,\beta,\widetilde{\omega}}$ for $r = 10$.

$|\omega^{(1)}_{\text{ref}} - \hat{\omega}| \approx 7.6 \cdot 10^{-9}$ between the refined value of the inner frequency and the computed value $\hat{\omega}$ for the average of $\{y^{(m)}\}_{m\geq 1}$ is, perhaps, larger than expected a priori (compare with the second row of results in table 3 for $r = 5$). We are more confident in the result for $\omega^{(1)}_{\text{ref}}$ than in that for $\hat{\omega}$. This larger than expected error for the average of the signal may explain why we get several spurious peaks in the sample $\{Z^2(2\pi\omega^{(j)})\}_{j=1}^{1000}$ that accumulate close to $\omega = 0$ (see figure 3 and the last 4 rows of table 5). The refined frequencies $\{\omega^{(j)}_{\text{ref}}\}_{j=12}^{15}$ in table 5 should be resonant with the first 11. We have been able to establish this fact for $j \in \{12, 13\}$, while for $j \in \{14, 15\}$ the corresponding Fourier coefficients are so small that we do not expect too much accuracy for them. Specifically, we have:

$$\omega^{(12)}_{\text{ref}} \approx \omega^{(5)}_{\text{ref}} - \omega^{(1)}_{\text{ref}}, \qquad \omega^{(13)}_{\text{ref}} \approx 3\omega^{(1)}_{\text{ref}} - \omega^{(2)}_{\text{ref}} - \omega^{(3)}_{\text{ref}} + \omega^{(7)}_{\text{ref}} + \omega^{(11)}_{\text{ref}} - \omega^{(13)}_{\text{ref}} - 1.$$

The error associated with each of these resonances is shown in the corresponding entry in the last column of table 5. Finally, we have computed by averaging and extrapolation the Fourier coefficients of the signal $\{y^{(m)}\}_{m\geq 1}$ up to order 4. In this case, the corresponding residuals $m^{(n)}$ behave worse than those for the selected torus for $r = 5$. Concretely, we obtain $m^{(0)} = 3.1 \cdot 10^{-2}$, $m^{(1)} = 3.9 \cdot 10^{-3}$, $m^{(2)} = 2.8 \cdot 10^{-3}$, $m^{(3)} = 2.4 \cdot 10^{-3}$, and $m^{(4)} = 2.1 \cdot 10^{-3}$.

References

[1] H.W. Broer, G.B. Huitema, and M.B. Sevryuk. *Quasi-periodic motions in families of dynamical systems. Order amidst chaos*. Lecture Notes in Math., Vol 1645. Springer-Verlag, Berlin, 1996.

[2] H.W. Broer and M.B. Sevryuk. KAM theory: Quasi-periodicity in dynamical systems. In *Handbook of Dynamical Systems*, volume 3C, pages 249–344. Elsevier, 2010.

[3] S. Das, C.B. Dock, Y. Saiki, M. Salgado-Flores, E. Sander, J. Wu, and J.A. Yorke. Measuring quasiperiodicity. *EPL*, 114(4):40005, 2016.

[4] S. Das and J.A. Yorke. Super convergence of ergodic averages for quasiperiodic orbits. *Nonlinearity*, 31(2):491–501, 2018.

[5] R. de la Llave. A tutorial on KAM theory. In *Smooth ergodic theory and its applications (Seattle, WA, 1999)*, volume 69 of *Proc. Sympos. Pure Math.*, pages 175–292. Amer. Math. Soc., Providence, RI, 2001.

[6] G. Gómez, J.-M. Mondelo, and C. Simó. A collocation method for the numerical Fourier analysis of quasi-periodic functions. I. Numerical tests and examples. *Discrete Contin. Dyn. Syst. Ser. B*, 14(1):41–74, 2010.

[7] G. Gómez, J.-M. Mondelo, and C. Simó. A collocation method for the numerical Fourier analysis of quasi-periodic functions. II. Analytical error estimates. *Discrete Contin. Dyn. Syst. Ser. B*, 14(1):75–109, 2010.

[8] À. Jorba, R. Ramírez-Ros, and J. Villanueva. Effective reducibility of quasi-periodic linear equations close to constant coefficients. *SIAM J. Math. Anal.*, 28(1):178–188, 1997.

[9] À. Jorba and J. Villanueva. On the normal behaviour of partially elliptic lower-dimensional tori of Hamiltonian systems. *Nonlinearity*, 10(4):783–822, 1997.

[10] J. Laskar. The chaotic motion of the solar system. A numerical estimate of the size of the chaotic zones. *Icarus*, 88:266–291, 1990.

[11] J. Laskar. Introduction to frequency map analysis. In *Hamiltonian systems with three or more degrees of freedom (S'Agaró, 1995)*, volume 533 of *NATO Adv. Sci. Inst. Ser. C Math. Phys. Sci.*, pages 134–150. Kluwer Acad. Publ., Dordrecht, 1999.

[12] J. Laskar, C. Froeschlé, and A. Celletti. The measure of chaos by the numerical analysis of the fundamental frequencies. Application to the standard mapping. *Phys. D*, 56(2-3):253–269, 1992.

[13] A. Luque and J. Villanueva. Computation of derivatives of the rotation number for parametric families of circle diffeomorphisms. *Phys. D*, 237(20):2599–2615, 2008.

[14] A. Luque and J Villanueva. Numerical computation of rotation numbers for quasi-periodic planar curves. *Phys. D*, 238(20):2025–2044, 2009.

[15] A. Luque and J. Villanueva. Quasi-periodic frequency analysis using averaging-extrapolation methods. *SIAM J. Appl. Dyn. Syst.*, 13(1):1–46, 2014.

[16] A. Luque and J. Villanueva. A numerical method for computing initial conditions of Lagrangian invariant tori using the frequency map. *Phys. D*, 325:63–73, 2016.

[17] J.D. Meiss and E. Sander. Birkhoff averages and the breakdown of invariant tori in volume-preserving maps. *Phys. D*, 428:Paper No. 133048, 20, 2021.

[18] E. Sander and J. D. Meiss. Birkhoff averages and rotational invariant circles for area-preserving maps. *Phys. D*, 411:132569, 19, 2020.

[19] T.M. Seara and J. Villanueva. On the numerical computation of Diophantine rotation numbers of analytic circle maps. *Phys. D*, 217(2):107–120, 2006.

A Some technical details

Throughout this section, we use notations, definitions and assumptions of section 2. The starting point is as described in remark 2.3. Our main purpose is to provide the details on the validity of formula (8) and, by extension, of formulas (6) (for $\bar{\omega} = 0$) and (7) (for $\bar{\omega} = \omega_0$), which correspond to the cases $\varepsilon = 0$.

To achieve these aims, we select an averaging order $p \geq 1$, and use recurrences in definition 2.2 to compute $S_n^l = S_n^l(\{x_m \mathrm{e}^{-\mathrm{i}m\bar{\omega}}\}_{m=1}^N)$, for any $n = 1, \ldots, N$ and $l = 0, \ldots, p$. Leaving aside any issue about convergence, it is not difficult to establish by induction the following formal expression for these sums (in terms of the Fourier coefficients of γ):

$$S_n^l = \sum_{k \in \mathbb{Z}^r} \hat{\gamma}_k F_n^l(\lambda_k \bar{\lambda}^{-1}). \tag{22}$$

To simplify formula (22), we have introduced the notations $\lambda_k = \mathrm{e}^{\mathrm{i}\langle k, \omega \rangle}$ and $\bar{\lambda} = \mathrm{e}^{\mathrm{i}\bar{\omega}}$, and we have defined

$$F_n^l(x) = \frac{x^l}{(x-1)^l}(x^n - 1) - \sum_{s=1}^{l-1} \binom{n+l-s-1}{l-s} \frac{x^s}{(x-1)^s}.$$

We note that by setting $x_m = 1$, $\forall m$, it is not difficult to verify that $F_n^l(1) = S_n^l(\{x_m\}_{m=1}^N) = \binom{n+l-1}{l}$. We set $l = p$ and rewrite formula (22) as follows:

$$S_n^p = \hat{\gamma}_{k_0} F_n^p(\lambda_{k_0} \bar{\lambda}^{-1}) - \sum_{s=1}^{p-1} \binom{n+p-s-1}{p-s} A_s^p + e_n^p, \tag{23}$$

where

$$A_s^p = \sum_{k \in \mathbb{Z}^r \setminus \{k_0\}} \hat{\gamma}_k \frac{(\lambda_k \bar{\lambda}^{-1})^s}{(\lambda_k \bar{\lambda}^{-1} - 1)^s}, \qquad e_n^p = \sum_{k \in \mathbb{Z}^r \setminus \{k_0\}} \hat{\gamma}_k \frac{(\lambda_k \bar{\lambda}^{-1})^p}{(\lambda_k \bar{\lambda}^{-1} - 1)^p}((\lambda_k \bar{\lambda}^{-1})^n - 1). \tag{24}$$

The motivation for writing S_n^p as in (23) is that, as $\lambda_{k_0} \bar{\lambda}^{-1} \approx 1$, then we expect $\hat{\gamma}_{k_0} F_n^p(\lambda_{k_0} \bar{\lambda}^{-1}) \approx \hat{\gamma}_{k_0} \binom{n+p-1}{p}$ to be the dominant term of this expression. Furthermore, $F_n^p(\lambda_{k_0} \bar{\lambda}^{-1}) \approx n^p/p!$ if $n \gg 1$.

Let us briefly discuss the convergence of expressions above. The simplest case is when $\bar{\omega} = \omega_0$ (i.e., $\varepsilon = 0$). Then, Diophantine conditions (1) for ω imply that $|\lambda_k \bar{\lambda}^{-1} - 1| \geq C|k - k_0|^{-\tau}$, $\forall k \neq k_0$. This lower bound on the denominators of A_s^p and e_n^p in (24), along with the analyticity of γ (see (2)), guarantee the convergence of these expressions and allows to derive an upper bound for the size of e_n^p independent of n. If $0 < \varepsilon \ll 1$, then it is not difficult to prove that we still have a Diophantine condition of the form $|\lambda_k \bar{\lambda}^{-1} - 1| \geq (C/2)|k - k_0|^{-\tau}$, $\forall k \neq k_0$, except for a Cantor-like set of values of $\bar{\omega}$ of small Lebesgue measure. For the values of $\bar{\omega}$ that verify this slightly worse Diophantine condition, the result for $\varepsilon \neq 0$ is

analogous to the result for $\varepsilon = 0$. For general values of $0 < \varepsilon \ll 1$, we can only ensure that the condition $|\lambda_k \bar{\lambda}^{-1} - 1| \geq (C/2)|k - k_0|^{-\tau}$ is satisfied up to very large values of $|k|_1$. Explicitly, if $|k - k_0| \leq c_1/\varepsilon^{1/\tau}$, for some $c_1 > 0$. Therefore, we only have a lower bound for the denominators in (24) related to such values of k. But if $|k - k_0| > c_1/\varepsilon^{1/\tau}$, then the analyticity of γ guarantees that the size of the Fourier coefficient $\hat{\gamma}_k$ is exponentially small on ε. This observation is the key point of the main result of [8], so the interested reader is referred there for further details. We split the contribution of γ to S_n^p into two parts. The first one collects the contribution of the coefficients $\hat{\gamma}_k$ for which $|k - k_0| \leq c_1/\varepsilon^{1/\tau}$ and the second one collects the contribution of those coefficients for which $|k - k_0| > c_1/\varepsilon^{1/\tau}$. To control the size of the first part, we rely on the Diophantine bounds for the denominators. To control the size of the second one, we simply multiply $|\hat{\gamma}_k|$ by a factor that takes into account the number of terms involved in the sum, rather than trying to bound the size of the sum by a geometric progression. We use this splitting to justify the validity of the following expression for the averaged sums $\widetilde{S}_n^p = p! S_n^p / n^p$:

$$\widetilde{S}_n^p = \hat{\gamma}_{k_0} \widetilde{F}_n^p(\lambda_{k_0} \bar{\lambda}^{-1}) + \sum_{s=1}^{p-1} \frac{\widetilde{A}_s^p}{n^s} + \widetilde{e}_n^p. \tag{25}$$

The constants $\{\widetilde{A}_s^p\}_{s=1}^{p-1}$ (independent of n) are defined in terms of the constants $\{A_s^p\}_{s=1}^{p-1}$, after redefining them by restricting the sums in (24) to $|k - k_0| \leq c_1/\varepsilon^{1/\tau}$. The new error term $\widetilde{e}_n^p$ is defined in terms of e_n^p and the part of the sums in (24) involving $\{A_s^p\}_{s=1}^{p-1}$ that is associated with $|k - k_0| \geq c_1/\varepsilon^{1/\tau}$. Finally, $\widetilde{F}_n^p = p! F_n^p / n^p$. Hence, for a fixed p, we have that $\widetilde{F}_n^p(\lambda_{k_0} \bar{\lambda}^{-1}) \approx 1$ if $\varepsilon \ll 1$ and $n \gg 1$. Furthermore, we have the following bound for the error term (we mainly highlight the contribution to it of the Diophantine constant C of (1)):

$$|\widetilde{e}_n^p| \leq \frac{\widetilde{C}_1}{C^p} \frac{1}{n^p} + \frac{\widetilde{C}_2}{\exp\left(\widetilde{c}_1/\varepsilon^{1/\tau}\right)}, \tag{26}$$

for some constants $\widetilde{C}_1$, $\widetilde{C}_2$ and $\widetilde{c}_1$ independent of n. Globally speaking, these constants only depend on r, τ, p, M, ρ and $|k_0|_1$. The idea of the presented averaging-extrapolation method is to ignore the contribution of $\widetilde{e}_n^p$ to formula (25) and to apply Richardson's extrapolation to the resulting expression. This allows to remove from it the contribution associated with the constants $\{\widetilde{A}_s^p\}_{s=1}^{p-1}$. More specifically, we fix p and N, and we select increasing positive integers $\{N_j\}_{j=1}^p$ behaving geometrically as those in definition 2.2, with $N_p = N$. We compute $\{\widetilde{S}_{N_j}^p\}_{j=1}^p$ and use these values to perform the extrapolation. To further describe the process, we introduce the following p-dimensional column vectors:

$$\mathcal{S} = (\widetilde{S}_{N_1}^p, \ldots, \widetilde{S}_{N_p}^p)^\top, \quad \mathcal{N}_s = (1/N_1^s, \ldots, 1/N_p^s)^\top, \quad \mathcal{F} = (\widetilde{F}_{N_1}^p, \ldots, \widetilde{F}_{N_p}^p)^\top, \quad \mathcal{E} = (\widetilde{e}_{N_1}^p, \ldots, \widetilde{e}_{N_p}^p)^\top,$$

for $s = 0, \ldots, p$. Then, we have established the following equation:

$$\mathcal{S} - \hat{\gamma}_{k_0} \mathcal{F}(\lambda_{k_0} \bar{\lambda}^{-1}) - \mathcal{E} = \sum_{s=1}^{p-1} \widetilde{A}_s^p \mathcal{N}_s.$$

As the vector defined by the rightmost part of this equality is linear combination of the vectors $\{\mathcal{N}_s\}_{s=1}^{p-1}$, then the $p \times p$ determinant that has these p vectors as columns must be zero. Consequently, we obtain:

$$\det(\mathcal{S}, \mathcal{N}_1, \ldots, \mathcal{N}_{p-1}) = \hat{\gamma}_{k_0} \Delta(\lambda_{k_0} \bar{\lambda}^{-1}) + \det(\mathcal{E}, \mathcal{N}_1, \ldots, \mathcal{N}_{p-1}), \tag{27}$$

where

$$\Delta = \det(\mathcal{F}, \mathcal{N}_1, \ldots, \mathcal{N}_{p-1}).$$

In particular, we observe that if we use

$$\widetilde{F}_n^p(1) = \frac{p!}{n^p}\binom{n+p-1}{p} = \frac{(n+p-1)(n+p-2)\cdots(n+1)n}{n^p},$$

then it is not difficult to show that the value of $\Delta(1)$ is given by the following Vandermonde determinant:

$$\Delta(1) = \det(\mathcal{N}_0, \mathcal{N}_1, \ldots, \mathcal{N}_{p-1}) = \prod_{\substack{s_1,s_2=1,\ldots,p \\ s_1>s_2}} \left(\frac{1}{N_{s_1}} - \frac{1}{N_{s_2}}\right) = \frac{1}{(N_1\cdots N_p)^{p-1}} \prod_{\substack{s_1,s_2=1,\ldots,p \\ s_1>s_2}} (N_{s_2} - N_{s_1}).$$

Furthermore, we introduce the $(p-1)$-dimensional column vectors $\mathcal{N}_{s;l}$ and the $(p-1)\times(p-1)$ Vandermonde determinants Δ_l, for $s, l = 1, \ldots, p$, defined by the following expressions:

$$\begin{aligned} \mathcal{N}_{s;l} &= (1/N_1^s, \ldots, 1/N_{l-1}^s, 1/N_{l+1}^s, \ldots 1/N_p^s)^\top, \\ \Delta_l &= \det(\mathcal{N}_{1;l}, \ldots, \mathcal{N}_{p-1;l}) = \frac{1}{(N_1\cdots N_{l-1}N_{l+1}\cdots N_p)^{p-1}} \prod_{\substack{s_1,s_2=1,\ldots,p \\ l\neq s_1>s_2\neq l}} (N_{s_2} - N_{s_1}). \end{aligned}$$

From them, we have:

$$\det(\mathcal{S}, \mathcal{N}_1, \ldots, \mathcal{N}_{p-1}) = \sum_{l=1}^{p} (-1)^{l+1}\Delta_l \widetilde{S}_{N_l}^p, \qquad \det(\mathcal{E}, \mathcal{N}_1, \ldots, \mathcal{N}_{p-1}) = \sum_{l=1}^{p} (-1)^{l+1}\Delta_l \widetilde{e}_{N_l}^p.$$

If we divide equation (27) by $\Delta(1)$, then we have established the following formula:

$$\sum_{l=1}^{p} (-1)^{l+1}\frac{\Delta_l}{\Delta(1)}\widetilde{S}_{N_l}^p = \hat{\gamma}_{k_0}\frac{\Delta(\lambda_{k_0}\bar{\lambda}^{-1})}{\Delta(1)} + \sum_{l=1}^{p} (-1)^{l+1}\frac{\Delta_l}{\Delta(1)}\widetilde{e}_{N_l}^p. \tag{28}$$

Simple computations show that if we set $c_l^p = (-1)^{l+1}\Delta_l/\Delta(1)$, then the coefficients $c_l^p = c_l^p(\{N_j\}_{j=1}^p)$ are given by formula (3). Consequently, we have established formula (8) for the extrapolation operator $\Theta_{\{N_j\}}^p$, where $\widetilde{\Delta}_{\{N_j\}} = \widetilde{\Delta}$ and the error term $\widetilde{E}$ are given by:

$$\widetilde{\Delta}(\mathrm{e}^{\mathrm{i}(\omega_0-\bar{\omega})}) = \widetilde{\Delta}(\lambda_{k_0}\bar{\lambda}^{-1}) = \frac{\Delta(\lambda_{k_0}\bar{\lambda}^{-1})}{\Delta(1)}, \qquad \widetilde{E} = \sum_{l=1}^{p} c_l^p \widetilde{e}_{N_l}^p. \tag{29}$$

We note that the function $\widetilde{\Delta}$ only depends on the selected integers $\{N_j\}_{j=1}^p$ and that $\widetilde{\Delta}(1) = 1$. According to definition 2.2, the integers $\{N_j\}_{j=1}^p$ verify $N_j \sim \mu^{p-j}N$, for some $0 < \mu < 1$. Consequently, the size of the coeficients $\{c_j^p\}_{j=1}^p$ given by (3) can be bounded, in terms of μ, by an expression independent of the selected $N_p = N$. Then, using (26), we conclude that $\widetilde{E}$ verifies a bound like the one given in (9), by re-defining the values of the constants $\widetilde{C}_1$ and $\widetilde{C}_2$ in (26), that now also depend on μ.